

# Supporting Information

## Trifluoroethylamine-substituted solvatochromic fluorophores exhibit polarity-insensitive high brightness

Ning Xu,<sup>a,b</sup> Qinglong Qiao,<sup>\*a</sup> Jie Chen,<sup>a</sup> Yi Tao,<sup>a</sup> Pengjun Bao,<sup>a</sup> Yinchan Zhang,<sup>a</sup> Jin Li<sup>a</sup> and  
Zhaochao Xu<sup>\*a,b</sup>

<sup>a</sup>CAS Key Laboratory of Separation Science for Analytical Chemistry, Dalian Institute of Chemical  
Physics, Chinese Academy of Sciences, Dalian University of Technology, 457 Zhongshan Road,  
Dalian 116023, China

<sup>b</sup>School of Chemistry, Dalian University of Technology, 2 Linggong Road, Dalian 116024, China

## Contents

1 Materials and Methods.....	2
1.1 Materials and instrument.....	2
1.2 Spectroscopic studies.....	2
1.3 Cell culture and transfection.....	3
1.4 Confocal imaging.....	3
1.5 Fluorescence recovery after photobleaching (FRAP) imaging.....	3
1.6 SIM imaging.....	3
2 Synthesis procedures.....	4
2.1 Synthesis of TFEA-Naph.....	4
2.2 Synthesis of TFEA-Cou.....	4
2.3 Synthesis of TFEA-NBD.....	5
2.4 Synthesis of TFEA-Naph-1.....	5
2.5 Synthesis of TFEA-Naph-2.....	6
2.6 Synthesis of TFEA-Naph-3.....	7
2.7 Synthesis of TFEA-Naph-Halo.....	8
3 Spectral characteristics.....	9
4 Imaging details.....	20
5 Spectra characterization.....	25

# 1 Materials and Methods

## 1.1 Materials and instrument

Unless otherwise specifically stated, all reagents were purchased from commercial suppliers (Sigma-Aldrich, J&K, Innochem and Aladdin) and used without further purification. Solvents [dimethyl sulfoxide (DMSO), dimethylformamide (DMF), methanol, ethanol, methanol, acetonitrile] were purchased from J&K and used without further treatment or distillation. Silica gel (200-300 mesh) was purchased from Innochem.

All  $^1\text{H}$ -NMR and  $^{13}\text{C}$ -NMR spectra were recorded on a Bruker 400 spectrometer with TMS as an internal standard. Chemical shifts were given in ppm and coupling constants (J) in Hz. High resolution mass spectrometry data were obtained with a HP1100LC/MSD mass spectrometer and a LC/Q-TOF MS spectrometer.

UV-vis absorption spectra were collected on an Agilent Cary 60 UV-Vis Spectrophotometer. Fluorescence measurements were performed on an Agilent CARY Eclipse fluorescence spectrophotometer.

Confocal images were performed on Olympus FV1000MPE with a microscope IX 71, a  $100\times$  / NA 1.40 oil objective lens, LU-NV series laser unit (laser combination: 405 nm; 543 nm; 488 nm; 635 nm). Super-resolution images were performed by Nikon N-STORM/SIM 5.0 Super-Resolution Microscope System with a motorized inverted microscope ECLIPSE Ti2-E, a  $100\times$  / NA 1.49 oil immersion TIRF objective lens (CFI HP), LU-NV series laser unit (405 nm, 488 nm, 561 nm, 647 nm), and an ORCA-Flash 4.0 sCMOS camera (Hamamatsu Photonics K.K.).

## 1.2 Spectroscopic studies

The probe stock solutions were firstly prepared as 2 mM stock solution in DMSO. Samples for spectroscopic analysis were prepared through diluting the stock solution in respective solvents. The concentration of samples was usually prepared at 5  $\mu\text{M}$ , unless stated otherwise.

For fluorescence quantum yield measurements, Coumarin 153 was used as a reference ( $\phi F_{(S)} = 0.53$  in in ethyl alcohol), and the quantum yield was calculated using the following equation.

$$\phi F_{(X)} = \phi F_{(S)} \cdot (A_S F_X / A_X F_S) (\eta_X / \eta_S)^2$$

Where  $\phi F$ , A and F represent the fluorescence quantum yield, the absorbance at the excitation wavelength and the area under the corrected emission curve, respectively. And  $\eta$  is the refractive index of the solvent. Subscripts X and S refer to the unknown and the standard.

The Lippert–Mataga theory describes the solvent dependency of spectral shifts as given in equation below:

$$\Delta\nu = \nu_a - \nu_e = \frac{1}{\lambda_{abs}^{max}} - \frac{1}{\lambda_{em}^{max}} \quad \text{and} \quad \Delta f = \left( \frac{\epsilon-1}{2\epsilon+1} - \frac{\eta^2-1}{2\eta^2+1} \right)$$

This equation shows that the Stokes shift ( $\Delta\nu$ ) depends on the dielectric constant ( $\epsilon$ ) and the refractive

index ( $\eta$ ) of the corresponding solvent.  $\nu_a$  and  $\nu_e$  represent the wavenumbers of the absorption and the fluorescence emission, respectively.  $\Delta f$  is the orientation polarizability of the solvent. Plotting the Stokes shift as a function of the orientation polarizability of the solvents gives the Lippert–Mataga plot.

### 1.3 Cell culture and transfection

HeLa cells were purchased from Cell Bank of Type Culture Collection of Chinese Academy of Sciences. Cells were maintained in Dulbecco's modified Eagle's medium (DMEM, Gibco) supplemented with 10% fetal bovine serum (FBS, Hyclone) which were cultured in a humidified atmosphere of 5% CO<sub>2</sub>/95% air at 37 °C. Before the imaging experiments, cells were seeded on glass bottom cell culture dish (Nest, polystyrene,  $\Phi$  15 mm) for 1-2 days to reach 50-80% confluency. The cells were then used for further experiments.

Transfection experiments were performed according to the manufacturer's protocol for Lipofectamine 2000 (Invitrogen). Briefly, 2  $\mu$ L of Lipofectamine 2000 (Invitrogen) and the plasmid were first diluted in 20  $\mu$ L of DMEM (Dulbecco's Modified Eagle's Medium). After 5 minutes, the plasmid diluted in 20  $\mu$ L DMEM was added to the diluted Lipofectamine 2000 (Invitrogen) and mixed gently. After another 10 minutes, the mixture was added to cell-cultured dish in 1 mL DMEM. The final plasmid concentration was controlled at 500-1000 ng/mL. After incubation at 37°C for 4 hours, the medium was changed from DMEM to DMEM containing 10% FBS. Transfected cells were used for confocal imaging 24-48 hours later.

### 1.4 Confocal imaging

The live HeLa cells were incubated with 0.5-3  $\mu$ M probes for 0.5-1 h at 37 °C in a 5% CO<sub>2</sub> atmosphere. The cells were then directly imaged using confocal microscopy without washing steps. Ex: 405 nm; collected: 415-465 nm, 425-475 nm, 425-500 nm, 425-525 nm, 450-550 nm, 500-600 nm for **TFEA-Naph** and **TFEA-Naph-Halo**. Ex: 488 nm; collected: 500-600 nm for **TFEA-Cou**. Ex: 770 nm; collected: 380-560 nm for **TFEA-NBD**. In co-localization experiments, lipid droplets were labeled by commercial dye LD 540.

The live HeLa cells, transfected with Halo-H2B or Halo-Tommon20, were incubated with 0.3-1  $\mu$ M **TFEA-Naph-Halo** for 0.5-1 h at 37 °C in a 5% CO<sub>2</sub> atmosphere, and then directly imaged using confocal microscopy without washing steps.

### 1.5 Fluorescence recovery after photobleaching (FRAP) imaging

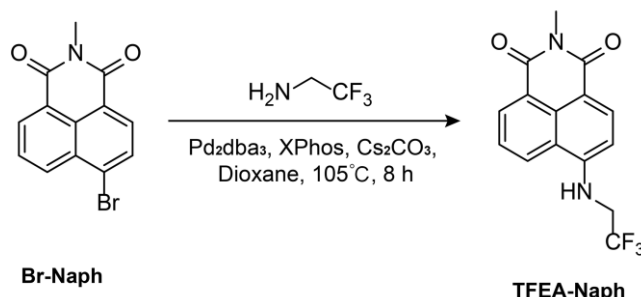
Fluorescence recovery after photobleaching (FRAP) experiments were carried out on Olympus FV1000 MPE confocal laser scanning microscope. Two images were taken before the bleach pulse and 30 images after the bleaching of regions of interest (ROIs). For photobleaching process, the ROIs were bleached by laser for 10 seconds. The fluorescence intensity was acquired by the software in imaging system.

### 1.6 SIM imaging

The live HeLa cells were incubated with 0.5  $\mu$ M **TFEA-Naph-Halo** for 1 h at 37 °C in a 5% CO<sub>2</sub> atmosphere, and then were directly imaged using super resolution microscopy without washing steps.

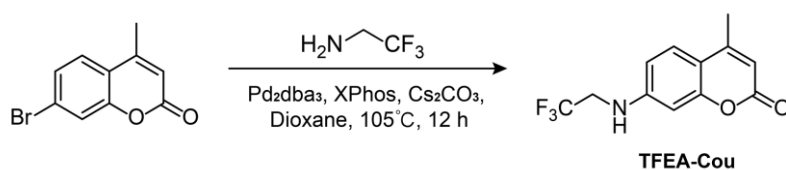
## 2 Synthesis procedures

### 2.1 Synthesis of TFEA-Naph



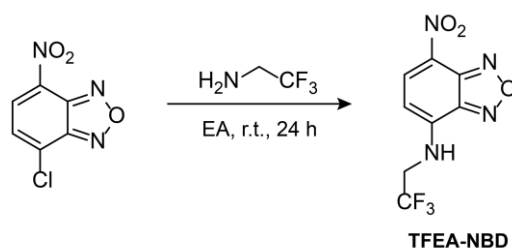
A two-neck bottle was charged with *N*-methyl-4-Bromo-1,8-naphthalimide (74 mg, 0.25 mmol), Pd<sub>2</sub>dba<sub>3</sub> (11 mg, 0.0125 mmol, 0.05 eq), XPhos (18 mg, 0.0375 mmol, 0.15 eq), and Cs<sub>2</sub>CO<sub>3</sub> (244 mg, 0.75 mmol, 3 eq). The two-neck bottle was sealed and evacuated/backfilled with nitrogen (3×). Then, 2,2,2-trifluoroethylamine (75 mg, 0.75 mmol, 3 eq) and 1,4-dioxane (10 mL) was added, the reaction was stirred at 105 °C for 8 h. It was then cooled to room temperature. The solvent was removed under reduced pressure and the residue was further purified by flash column chromatography (DCM:MeOH = 50:1) to afford 51 mg of yellow powder, yield 66%. <sup>1</sup>H NMR (400 MHz, DMSO) δ 8.66 (d, *J* = 8.4 Hz, 1H), 8.41 (d, *J* = 7.0 Hz, 1H), 8.26 (d, *J* = 8.5 Hz, 1H), 8.00 (s, 1H), 7.78 (m, 1H), 7.08 (d, *J* = 8.5 Hz, 1H), 4.34 (dd, *J* = 9.1, 5.6 Hz, 2H), 3.35 (s, 3H). <sup>13</sup>C NMR (400 MHz, DMSO) δ 164.35, 163.58, 149.99, 133.85, 131.12, 129.38, 128.64, 125.39, 122.48, 120.71, 110.47, 105.40, 26.84. HRMS (ESI) calcd for C<sub>15</sub>H<sub>12</sub>F<sub>3</sub>N<sub>2</sub>O<sub>2</sub><sup>+</sup> [M+H]<sup>+</sup> 309.0845, found 309.0844.

### 2.2 Synthesis of TFEA-Cou



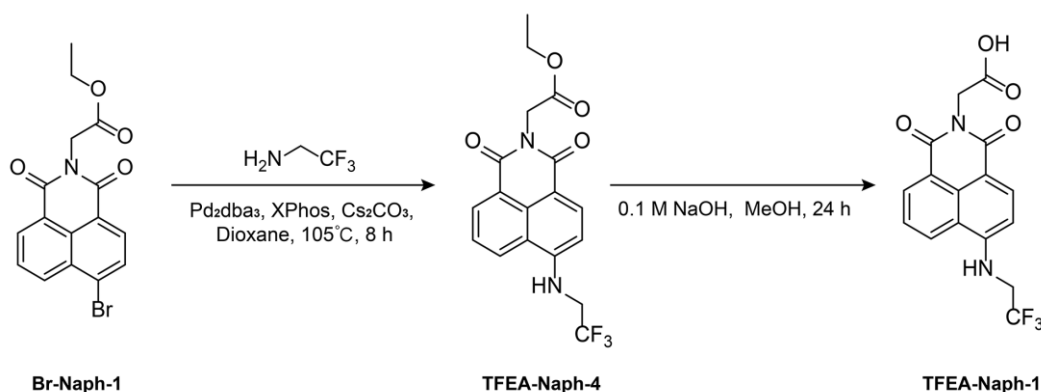
A two-neck bottle was charged with 7-Bromo-4-methylcoumarin (119 mg, 0.5 mmol), Pd<sub>2</sub>dba<sub>3</sub> (23 mg, 0.025 mmol, 0.05 eq), XPhos (36 mg, 0.075 mmol, 0.15 eq), and Cs<sub>2</sub>CO<sub>3</sub> (487 mg, 1.5 mmol, 3 eq). The two-neck bottle was sealed and evacuated/backfilled with nitrogen (3×). Then, 2,2,2-trifluoroethylamine (150 mg, 1.5 mmol, 3 eq) and 1,4-dioxane (10 mL) was added, the reaction was stirred at 105 °C for 12 h. It was then cooled to room temperature. The solvent was removed under reduced pressure and the residue was further purified by flash column chromatography (DCM) to afford 54 mg powder, yield 42%. <sup>1</sup>H NMR (400 MHz, DMSO) δ 7.50 (d, *J* = 8.6 Hz, 1H), 7.12 (s, 1H), 6.78 (d, *J* = 8.1 Hz, 1H), 6.71 (s, 1H), 6.01 (s, 1H), 4.20 (m, 2H), 2.34 (s, 3H). <sup>13</sup>C NMR (400 MHz, DMSO) δ 161.00, 155.76, 154.09, 151.89, 126.60, 110.82, 110.53, 109.14, 98.07, 43.96, 43.63, 18.48. HRMS (ESI) calcd for C<sub>12</sub>H<sub>11</sub>F<sub>3</sub>NO<sub>2</sub><sup>+</sup> [M+H]<sup>+</sup> 258.0736, found 258.0746.

## 2.3 Synthesis of TFEA-NBD



A flask was charged with 4-chloro-7-nitrobenzofurazan (50 mg, 0.25 mmol), 2,2,2-trifluoroethylamine (75 mg, 0.75 mmol, 3 eq) and Ethyl acetate (10 mL). The mixture was stirred at room temperature for 24 h. And the solvent was removed under reduced pressure and the residue was further purified by flash column chromatography (DCM:MeOH = 40:1) to afford 52 mg of orange solid, yield 80%.  $^1\text{H}$  NMR (400 MHz, DMSO)  $\delta$  9.52 (s, 1H), 8.61 (d,  $J$  = 8.8 Hz, 1H), 6.76 (d,  $J$  = 8.8 Hz, 1H), 4.48 (dd,  $J$  = 17.9, 8.7 Hz, 2H).  $^{13}\text{C}$  NMR (400 MHz, DMSO)  $\delta$  145.03, 144.93, 144.37, 137.84, 123.93, 123.83, 101.75, 44.53. HRMS (ESI) calcd for  $\text{C}_8\text{H}_6\text{F}_3\text{N}_4\text{O}_3^+$   $[\text{M}+\text{H}]^+$  263.0387, found 263.0389.

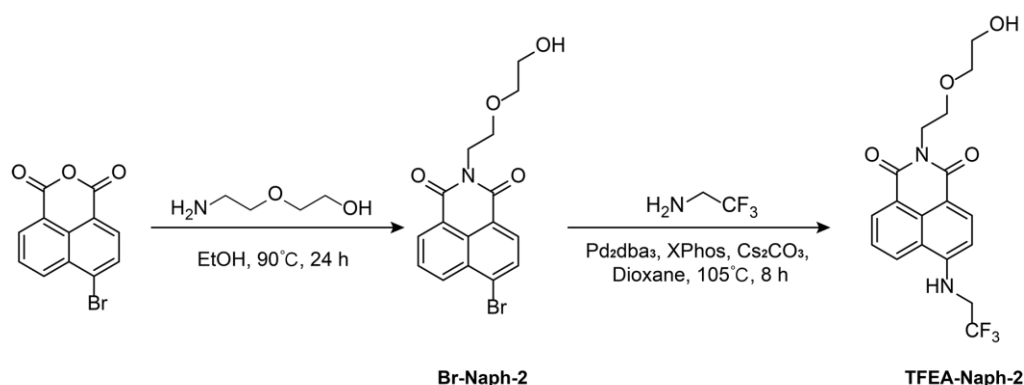
## 2.4 Synthesis of TFEA-Naph-1



**Synthesis of TFEA-Naph-4:** A two-neck bottle was charged with *N*-ethoxycarbonylmethyl-4-bromo-1,8-naphthalimide (120 mg, 0.33 mmol),  $\text{Pd}_2\text{dba}_3$  (15 mg, 0.0165 mmol, 0.05 eq), XPhos (24 mg, 0.017 mmol, 0.15 eq), and  $\text{Cs}_2\text{CO}_3$  (325 mg, 1 mmol, 3 eq). The two-neck bottle was sealed and evacuated/backfilled with nitrogen (3 $\times$ ). Then, 2,2,2-trifluoroethylamine (100 mg, 1 mmol, 3 eq) and 1,4-dioxane (10 mL) was added, the reaction was stirred at 105  $^\circ\text{C}$  for 8 h. It was then cooled to room temperature. The solvent was removed under reduced pressure and the residue was further purified by flash column chromatography (DCM:MeOH = 75:1) to afford 72 mg of yellow powder, yield 58%.  $^1\text{H}$  NMR (400 MHz, DMSO)  $\delta$  8.77 (d,  $J$  = 8.4 Hz, 1H), 8.49 (d,  $J$  = 7.2 Hz, 1H), 8.33 (d,  $J$  = 8.5 Hz, 1H), 8.17 (m, 1H), 7.79 (t,  $J$  = 7.9 Hz, 1H), 7.17 (d,  $J$  = 8.5 Hz, 1H), 4.78 (s, 2H), 4.46 (m, 2H), 4.15 (q,  $J$  = 7.0 Hz, 2H), 1.21 (t,  $J$  = 7.0 Hz, 3H).  $^{13}\text{C}$  NMR (101 MHz, DMSO)  $\delta$  168.73, 163.87, 162.92, 150.62, 134.47, 131.74, 129.74, 129.37, 125.67, 121.99, 120.84, 109.68, 105.73, 61.45, 41.39, 14.52. HRMS (ESI) calcd for  $\text{C}_{18}\text{H}_{16}\text{F}_3\text{N}_2\text{O}_4^+$   $[\text{M}+\text{H}]^+$  381.1057, found 381.1053.

**Synthesis of TFEA-Naph-1:** TFEA-Naph-4 (50 mg, 0.13 mmol) was solved in 5 mL MeOH, and 1 M NaOH (200  $\mu$ L, 0.2 mmol, 1.5 eq) was added. After stirring the reaction at room temperature for 24 h, it was acidified with 1 M HCl (240  $\mu$ L). The solvent was removed under reduced pressure and the residue was further purified by flash column chromatography (DCM:MeOH = 10:1) to afford 38 mg of yellow powder, yield 83%.  $^1\text{H}$  NMR (400 MHz, DMSO)  $\delta$  8.75 (d,  $J$  = 8.2 Hz, 1H), 8.48 (d,  $J$  = 6.9 Hz, 1H), 8.32 (d,  $J$  = 8.5 Hz, 1H), 8.14 (t,  $J$  = 6.5 Hz, 1H), 7.77 (dd,  $J$  = 8.2, 7.6 Hz, 1H), 7.15 (d,  $J$  = 8.6 Hz, 1H), 4.65 (s, 2H), 4.37 (m, 2H).  $^{13}\text{C}$  NMR (400 MHz, DMSO)  $\delta$  168.73, 163.87, 162.92, 150.62, 134.47, 131.74, 129.74, 129.37, 125.67, 121.99, 120.84, 109.68, 105.73, 61.45, 14.52. HRMS (ESI) calcd for  $\text{C}_{16}\text{H}_{12}\text{F}_3\text{N}_2\text{O}_4^+$   $[\text{M}+\text{H}]^+$  353.0744, found 353.0749.

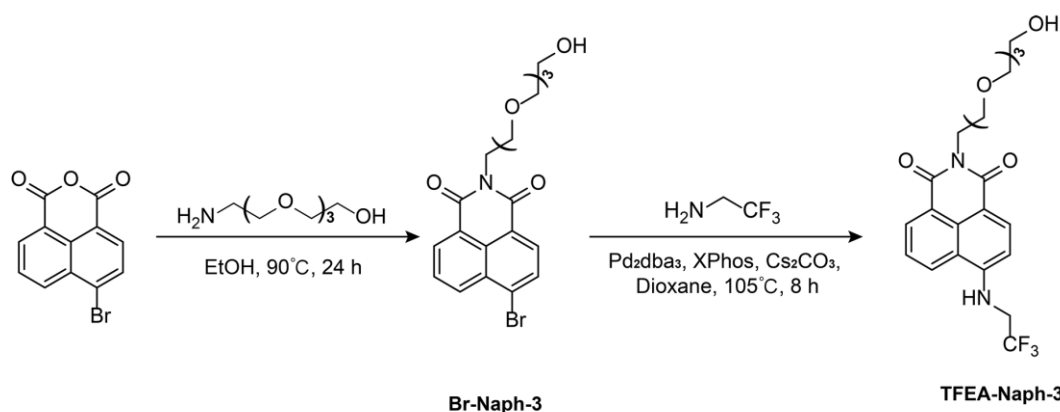
## 2.5 Synthesis of TFEA-Naph-2



**Synthesis of Br-Naph-2:** 4-Bromo-1,8-naphthalic anhydride (276 mg, 1 mmol), 2-(2-aminoethoxy)-ethanol (525 mg, 5 mmol, 5 eq.) were added into 50 mL ethanol. And the reaction was stirred at 90 °C for 24 h. It was then cooled to room temperature. The solvent was removed under reduced pressure and the residue was further purified by flash column chromatography (PE:DCM = 1:1) to afford 243 mg of white powder, yield 67%.  $^1\text{H}$  NMR (400 MHz,  $\text{CDCl}_3$ )  $\delta$  8.60(m, 1H), 8.44 (m, 1H), 8.30 (m, 1H), 7.99 (m, 1H), 7.71 (dd,  $J$  = 7.6, 5.7 Hz, 1H), 4.45 (m, 2H), 3.91 (m, 2H), 3.70 (d,  $J$  = 3.8 Hz, 2H), 3.67 (d,  $J$  = 3.6 Hz, 2H), 2.89 (s, 1H).  $^{13}\text{C}$  NMR (400 MHz,  $\text{CDCl}_3$ )  $\delta$  163.63, 133.15, 132.05, 131.21, 130.98, 130.26, 128.64, 127.97, 122.65, 121.79, 72.32, 68.28, 61.78, 39.61. HRMS (ESI) calcd for  $\text{C}_{16}\text{H}_{15}\text{BrNO}_4^+$   $[\text{M}+\text{H}]^+$  364.0179, found 364.0179.

**Synthesis of TFEA-Naph-2:** A two-neck bottle was charged with **Br-Naph-2** (180 mg, 0.5 mmol),  $\text{Pd}_2\text{dba}_3$  (23 mg, 0.025 mmol, 0.05 eq), XPhos (36 mg, 0.075 mmol, 0.15 eq), and  $\text{Cs}_2\text{CO}_3$  (487 mg, 1.5 mmol, 3 eq). The two-neck bottle was sealed and evacuated/backfilled with nitrogen (3 $\times$ ). Then, 2,2,2-trifluoroethylamine (150 mg, 1.5 mmol, 3 eq) and 1,4-dioxane (10 mL) was added, the reaction was stirred at 105 °C for 8 h. It was then cooled to room temperature. The solvent was removed under reduced pressure and the residue was further purified by flash column chromatography (DCM:MeOH = 40:1) to afford 99 mg of yellow powder, yield 52%.  $^1\text{H}$  NMR (400 MHz,  $\text{CDCl}_3$ )  $\delta$  8.26 (m, 2H), 7.99 (d,  $J$  = 8.1 Hz, 1H), 7.39 (t,  $J$  = 7.7 Hz, 1H), 6.57 (d,  $J$  = 8.2 Hz, 1H), 6.08 (s, 1H), 4.35 (s, 2H), 4.05 (m, 2H), 3.89 (s, 2H), 3.73 (s, 4H), 3.00 (s, 1H).  $^{13}\text{C}$  NMR (400 MHz,  $\text{CDCl}_3$ )  $\delta$  164.81, 164.55, 148.34, 133.78, 131.51, 129.13, 126.46, 125.22, 122.31, 120.18, 111.57, 104.72, 71.77, 68.52, 61.93, 39.02, 29.71. HRMS (ESI) calcd for  $\text{C}_{18}\text{H}_{18}\text{F}_3\text{N}_2\text{O}_4^+$   $[\text{M}+\text{H}]^+$  383.1213, found 383.1220.

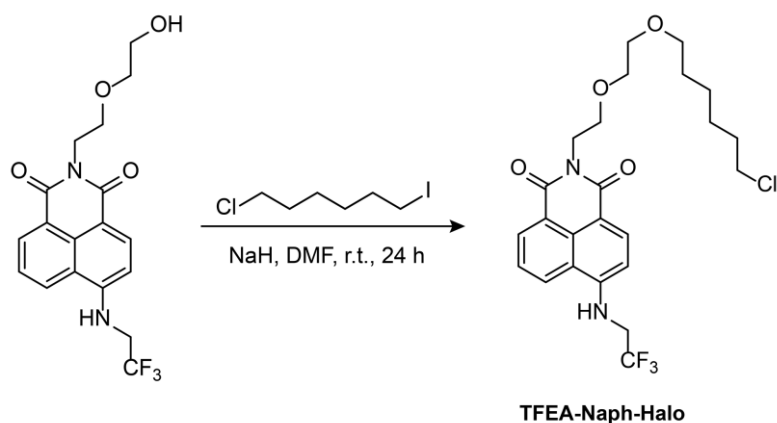
## 2.6 Synthesis of TFEA-Naph-3



**Synthesis of Br-Naph-3:** 4-Bromo-1,8-naphthalic anhydride (138 mg, 0.5 mmol), 1-Amino-3,6,9-trioxaundecan-11-ol (193 mg, 1 mmol, 2 eq.) were added into 50 mL ethanol. And the reaction was stirred at 90 °C for 24 h. It was then cooled to room temperature. The solvent was removed under reduced pressure and the residue was further purified by flash column chromatography (DCM) to afford 112 mg of white powder, yield 50%. <sup>1</sup>H NMR (400 MHz, CDCl<sub>3</sub>) δ 8.61 (d, *J* = 7.2 Hz, 1H), 8.51 (d, *J* = 8.5 Hz, 1H), 8.36 (d, *J* = 7.9 Hz, 1H), 8.00 (d, *J* = 7.9 Hz, 1H), 7.81 (dd, *J* = 8.2, 7.6 Hz, 1H), 4.42 (t, *J* = 6.0 Hz, 2H), 3.83 (t, *J* = 6.0 Hz, 2H), 3.69 (m, 4H), 3.63 (m, 2H), 3.59 (m, 4H), 3.56 (m, 2H). <sup>13</sup>C NMR (400 MHz, CDCl<sub>3</sub>) δ 163.60, 163.57, 133.23, 132.05, 131.23, 131.05, 130.49, 130.26, 128.91, 128.04, 122.93, 122.07, 77.41, 77.10, 76.78, 72.52, 70.59, 70.54, 70.27, 70.12, 67.91, 61.68, 39.27. HRMS (ESI) calcd for C<sub>20</sub>H<sub>23</sub>BrNO<sub>6</sub><sup>+</sup> [M+H]<sup>+</sup> 452.0703, found 452.0730.

**Synthesis of TFEA-Naph-3:** A two-neck bottle was charged with Br-Naph-3 (100 mg, 0.22 mmol), Pd<sub>2</sub>dba<sub>3</sub> (10 mg, 0.011 mmol, 0.05 eq), XPhos (16 mg, 0.033 mmol, 0.15 eq), and Cs<sub>2</sub>CO<sub>3</sub> (215 mg, 0.66 mmol, 3 eq). The two-neck bottle was sealed and evacuated/backfilled with nitrogen (3×). Then, 2,2,2-trifluoroethylamine (66 mg, 0.66 mmol, 3 eq) and 1,4-dioxane (10 mL) was added, the reaction was stirred at 105 °C for 8 h. It was then cooled to room temperature. The solvent was removed under reduced pressure and the residue was further purified by flash column chromatography (DCM:MeOH = 10:1) to afford 41 mg of yellow powder, yield 40%. <sup>1</sup>H NMR (400 MHz, DMSO) δ 8.71 (d, *J* = 8.0 Hz, 1H), 8.50 (m, 1H), 8.31 (d, *J* = 8.5 Hz, 1H), 8.12 (m, 1H), 7.76 (dd, *J* = 8.4, 7.4 Hz, 1H), 7.14 (d, *J* = 8.5 Hz, 1H), 4.54 (t, *J* = 5.5 Hz, 1H), 4.36 (m, 2H), 4.22 (t, *J* = 6.5 Hz, 2H), 3.64 (t, *J* = 6.4 Hz, 2H), 3.55 (m, 2H), 3.50 (m, 2H), 3.46 (m, 6H), 3.36 (m, 2H). <sup>13</sup>C NMR (400 MHz, DMSO) δ 164.18, 163.36, 150.16, 134.10, 131.40, 129.63, 128.85, 125.54, 122.52, 120.77, 110.35, 105.56, 72.78, 70.26, 70.16, 70.13, 70.07, 67.51, 60.64, 38.88. HRMS (ESI) calcd for C<sub>22</sub>H<sub>26</sub>F<sub>3</sub>N<sub>2</sub>O<sub>6</sub><sup>+</sup> [M+H]<sup>+</sup> 471.1737, found 471.1732.

## 2.7 Synthesis of TFEA-Naph-Halo



A Schlenk bottle was charged with TFEA-Naph-2 (65 mg, 0.17 mmol), NaH (4 mg, 0.17 mmol, 1 eq.), and the Schlenk bottle was sealed and evacuated/backfilled with nitrogen (3 $\times$ ). Then, 1-chloro-6-iodohexane (84 mg, 0.34 mmol, 2 eq.) and DMF (5 mL) was added, the reaction was stirred at 105  $^{\circ}$ C for 8 h. It was then cooled to room temperature. The solvent was removed under reduced pressure and the residue was further purified by flash column chromatography (DCM:MeOH = 100:1) to afford 28 mg of yellow powder, yield 33%.  $^1\text{H}$  NMR (400 MHz,  $\text{CDCl}_3$ )  $\delta$  8.57 (d,  $J$  = 7.2 Hz, 1H), 8.47 (d,  $J$  = 8.4 Hz, 1H), 8.13 (d,  $J$  = 8.4 Hz, 1H), 7.67 (t,  $J$  = 7.9 Hz, 1H), 6.87 (d,  $J$  = 8.4 Hz, 1H), 5.46 (s, 1H), 4.42 (t,  $J$  = 6.1 Hz, 2H), 4.17 (m, 2H), 3.84 (t,  $J$  = 6.1 Hz, 2H), 3.70 (m, 2H), 3.56 (m, 2H), 3.49 (t,  $J$  = 6.7 Hz, 2H), 3.39 (t,  $J$  = 6.6 Hz, 2H), 1.73 (m, 2H), 1.58 (m, 2H), 1.47 (m, 3H), 1.35 (m, 4H).  $^{13}\text{C}$  NMR (400 MHz,  $\text{CDCl}_3$ )  $\delta$  164.44, 147.47, 133.74, 133.24, 131.40, 127.32, 125.56, 123.30, 120.60, 112.85, 105.19, 100.00, 71.21, 70.23, 70.13, 68.09, 45.09, 39.00, 32.52, 31.94, 29.71, 29.46, 29.38, 26.70, 25.37, 22.71, 14.13. HRMS (ESI) calcd for  $\text{C}_{24}\text{H}_{29}\text{ClF}_3\text{N}_2\text{O}_4^+$   $[\text{M}+\text{H}]^+$  501.1762, found 501.1762.



### 3 Spectral characteristics

Table S1 Spectroscopic data of **TFEA-Naph** in various solvents: peak UV-vis absorption wavelength ( $\lambda_{\text{abs}}$ ), maximum emission wavelength ( $\lambda_{\text{em}}$ ), Stokes shifts, molar absorption coefficient ( $\epsilon$ ), fluorescence quantum yield ( $\phi$ ) and brightness.

Solvent	$\lambda_{\text{abs}}$ (nm)	$\lambda_{\text{em}}$ (nm)	$\Delta\lambda$ (nm)	$\epsilon$ ( $\text{M}^{-1}\text{cm}^{-1}$ )	$\phi$	Brightness ( $\text{M}^{-1}\text{cm}^{-1}$ )
Dioxane	401	476	75	12270	0.92	11288
PhMe	401	473	72	12400	0.81	10044
Ether	400	471	71	11690	0.95	11105
$\text{CHCl}_3$	403	483	80	11820	0.94	11110
EA	400	479	79	12320	0.82	10102
THF	407	478	71	13850	0.84	11634
DCM	401	482	81	10740	0.94	10095
Acetone	407	487	80	12120	0.88	10665
EtOH	415	503	88	14760	0.85	12546
MeOH	417	508	91	14150	0.80	11320
ACN	407	490	83	12860	0.84	10802
DMF	416	497	81	13290	0.83	11030
DMSO	421	503	82	13410	0.89	11934
$\text{H}_2\text{O}$	426	525	99	14690	0.50	7345
$\text{D}_2\text{O}$	423	523	100	12600	0.38	4788

Table S2 Spectroscopic data of **TFEA-Cou** in various solvents: peak UV-vis absorption wavelength ( $\lambda_{\text{abs}}$ ), maximum emission wavelength ( $\lambda_{\text{em}}$ ), Stokes shifts, molar absorption coefficient ( $\epsilon$ ), fluorescence quantum yield ( $\phi$ ) and brightness.

Solvent	$\lambda_{\text{abs}}$ (nm)	$\lambda_{\text{em}}$ (nm)	$\Delta\lambda$ (nm)	$\epsilon$ ( $\text{M}^{-1}\text{cm}^{-1}$ )	$\phi$	Brightness ( $\text{M}^{-1}\text{cm}^{-1}$ )
Dioxane	337	397	60	17684	0.75	13263
PhMe	337	396	59	17836	0.73	13020
Ether	335	396	61	16124	0.83	13382
$\text{CHCl}_3$	337	401	64	16018	0.88	14095
EA	336	399	63	18210	0.82	14932
THF	340	399	59	20300	0.83	16849
DCM	336	399	63	15260	0.91	13886
EtOH	349	419	70	20390	0.90	18351
MeOH	348	425	77	18636	0.80	14908
ACN	337	407	70	18734	0.85	15923
DMF	345	412	67	17600	0.92	16192
DMSO	349	413	64	17750	0.96	17040
$\text{H}_2\text{O}$	350	432	82	16258	0.94	15282

Table S3 Spectroscopic data of **TFEA-NBD** in various solvents: peak UV-vis absorption wavelength ( $\lambda_{\text{abs}}$ ), maximum emission wavelength ( $\lambda_{\text{em}}$ ), Stokes shifts, molar absorption coefficient ( $\epsilon$ ), fluorescence quantum yield ( $\phi$ ) and brightness.

Solvent	$\lambda_{\text{abs}}$ (nm)	$\lambda_{\text{em}}$ (nm)	$\Delta\lambda$ (nm)	$\epsilon$ ( $\text{M}^{-1}\text{cm}^{-1}$ )	$\phi$	Brightness ( $\text{M}^{-1}\text{cm}^{-1}$ )
Dioxane	429	509	80	16138	0.31	5000
PhMe	431	507	76	15352	0.32	4912
Ether	426	506	80	13278	0.21	2788
$\text{CHCl}_3$	425	507	82	14400	0.35	5054
EA	431	506	75	17150	0.42	7203
THF	435	506	71	18642	0.48	8948
DCM	428	508	80	14646	0.38	5565
Acetone	438	511	73	15970	0.59	9422
EtOH	443	513	70	21266	0.49	10420
MeOH	441	520	79	19110	0.44	8408
ACN	438	513	75	18718	0.58	10856
DMSO	461	528	67	19460	0.29	5643
$\text{H}_2\text{O}$	457	529	72	21360	0.067	1431
$\text{D}_2\text{O}$	457	527	70	20712	0.076	1574

Table S4 Spectroscopic data of **TFEA-Naph-1** in various solvents: peak UV-vis absorption wavelength ( $\lambda_{\text{abs}}$ ), maximum emission wavelength ( $\lambda_{\text{em}}$ ), Stokes shifts, molar absorption coefficient ( $\epsilon$ ), fluorescence quantum yield ( $\phi$ ) and brightness.

Solvent	$\lambda_{\text{abs}}$ (nm)	$\lambda_{\text{em}}$ (nm)	$\Delta\lambda$ (nm)	$\epsilon$ ( $\text{M}^{-1}\text{cm}^{-1}$ )	$\phi$	Brightness ( $\text{M}^{-1}\text{cm}^{-1}$ )
Dioxane	403	477	74	8370	0.95	7951
CHCl <sub>3</sub>	403	482	79	6878	0.83	5708
EtOH	418	501	83	9014	0.83	7481
MeOH	414	508	94	8694	0.75	6520
ACN	411	493	82	8436	0.75	6327
DMSO	422	504	82	8916	0.85	7616
H <sub>2</sub> O	427	522	95	9400	0.51	4794

Table S5 Spectroscopic data of **TFEA-Naph-2** in d various solvents: peak UV-vis absorption wavelength ( $\lambda_{\text{abs}}$ ), maximum emission wavelength ( $\lambda_{\text{em}}$ ), Stokes shifts, molar absorption coefficient ( $\epsilon$ ), fluorescence quantum yield ( $\phi$ ) and brightness.

Solvent	$\lambda_{\text{abs}}$ (nm)	$\lambda_{\text{em}}$ (nm)	$\Delta\lambda$ (nm)	$\epsilon$ ( $\text{M}^{-1}\text{cm}^{-1}$ )	$\phi$	Brightness ( $\text{M}^{-1}\text{cm}^{-1}$ )
Dioxane	401	479	78	9960	0.93	9262
CHCl <sub>3</sub>	405	483	78	9276	0.94	8728
EtOH	417	503	86	11230	0.79	8871
MeOH	416	506	90	11520	0.73	8409
ACN	409	496	97	10380	0.81	8407
DMSO	422	503	81	10900	0.87	9483
H <sub>2</sub> O	426	526	100	11590	0.46	5331

Table S6 Spectroscopic data of **TFEA-Naph-3** in various solvents: peak UV-vis absorption wavelength ( $\lambda_{\text{abs}}$ ), maximum emission wavelength ( $\lambda_{\text{em}}$ ), Stokes shifts, molar absorption coefficient ( $\epsilon$ ), fluorescence quantum yield ( $\phi$ ) and brightness.

Solvent	$\lambda_{\text{abs}}$ (nm)	$\lambda_{\text{em}}$ (nm)	$\Delta\lambda$ (nm)	$\epsilon$ ( $\text{M}^{-1}\text{cm}^{-1}$ )	$\phi$	Brightness ( $\text{M}^{-1}\text{cm}^{-1}$ )
Dioxane	404	481	77	9800	0.93	9114
CHCl <sub>3</sub>	403	480	77	10618	0.91	9662
EtOH	418	500	82	10742	0.80	8593
MeOH	416	508	92	10876	0.74	8048
ACN	408	494	86	10748	0.79	8490
DMSO	433	504	71	11088	0.83	9203
H <sub>2</sub> O	427	521	94	10790	0.50	5395

Table S7 Spectroscopic data of **TFEA-NBD** in water/DMSO system: peak UV-vis absorption wavelength ( $\lambda_{abs}$ ), maximum emission wavelength ( $\lambda_{em}$ ), Stokes shifts, molar absorption coefficient ( $\epsilon$ ) and fluorescence quantum yield ( $\phi$ ).

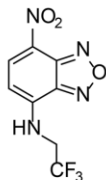
Fluorophore	Solvent	$\lambda_{abs}$ (nm)	$\lambda_{em}$ (nm)	$\Delta\lambda$ (nm)	$\epsilon$ ( $M^{-1}cm^{-1}$ )	$\phi$
	H <sub>2</sub> O/DMSO (95%/5%)	455	526	71	21504	0.077
	H <sub>2</sub> O/DMSO (90%/10%)	455	527	72	21210	0.086
	H <sub>2</sub> O/DMSO (50%/50%)	457	529	72	20800	0.224

Table S8 Detailed photophysical data of TFEA-Naph in the different solvents

Solvents	$\epsilon$	$n$	$f_{(\epsilon,n)}$	$\lambda_{abs}$ (nm)	$\lambda_{em}$ (nm)	$\nu_a$ ( $cm^{-1}$ )	$\nu_e$ ( $cm^{-1}$ )	$\nu_a-\nu_e$ ( $cm^{-1}$ )
Dioxnae	2.25	1.422	0.025	401	476	$2.494 \times 10^4$	$2.101 \times 10^4$	$3.93 \times 10^3$
CHCl <sub>3</sub>	4.81	1.446	0.148	403	483	$2.481 \times 10^4$	$2.070 \times 10^4$	$4.11 \times 10^3$
DCM	8.93	1.424	0.217	401	482	$2.494 \times 10^4$	$2.075 \times 10^4$	$4.19 \times 10^3$
Acetone	20.7	1.359	0.284	407	487	$2.457 \times 10^4$	$2.053 \times 10^4$	$4.04 \times 10^3$
EtOH	24.5	1.361	0.289	415	503	$2.410 \times 10^4$	$1.988 \times 10^4$	$4.22 \times 10^3$
MeOH	32.7	1.328	0.309	417	508	$2.398 \times 10^4$	$1.969 \times 10^4$	$4.29 \times 10^3$
DMF	37	1.427	0.276	416	497	$2.404 \times 10^4$	$2.012 \times 10^4$	$3.92 \times 10^3$
ACN	37.5	1.344	0.305	407	490	$2.457 \times 10^4$	$2.041 \times 10^4$	$4.16 \times 10^3$
DMSO	46.7	1.478	0.263	421	503	$2.375 \times 10^4$	$1.988 \times 10^4$	$3.87 \times 10^3$

Table S9 Detailed photophysical data of TFEA-Cou in the different solvents

Solvents	$\epsilon$	$n$	$f(\epsilon, n)$	$\lambda_{abs}$ (nm)	$\lambda_{em}$ (nm)	$\nu_a$ ( $\text{cm}^{-1}$ )	$\nu_e$ ( $\text{cm}^{-1}$ )	$\nu_a - \nu_e$ ( $\text{cm}^{-1}$ )
Dioxnae	2.25	1.422	0.025	337	397	$2.967 \times 10^4$	$2.519 \times 10^4$	$4.48 \times 10^3$
Ethyl ether	4.34	1.352	0.167	335	396	$2.985 \times 10^4$	$2.525 \times 10^4$	$4.60 \times 10^3$
$\text{CHCl}_3$	4.81	1.446	0.148	337	401	$2.967 \times 10^4$	$2.494 \times 10^4$	$4.73 \times 10^3$
DCM	8.93	1.424	0.217	336	399	$2.976 \times 10^4$	$2.506 \times 10^4$	$4.70 \times 10^3$
EtOH	24.5	1.361	0.289	349	419	$2.865 \times 10^4$	$2.387 \times 10^4$	$4.78 \times 10^3$
MeOH	32.7	1.328	0.309	348	425	$2.874 \times 10^4$	$2.353 \times 10^4$	$5.21 \times 10^3$
DMF	37	1.427	0.276	345	412	$2.899 \times 10^4$	$2.427 \times 10^4$	$4.72 \times 10^3$
ACN	37.5	1.344	0.305	337	407	$2.967 \times 10^4$	$2.457 \times 10^4$	$5.10 \times 10^3$
DMSO	46.7	1.478	0.263	349	413	$2.865 \times 10^4$	$2.421 \times 10^4$	$4.44 \times 10^3$

Table S10 Detailed photophysical data of TFEA-NBD in the different solvents

Solvents	$\epsilon$	$n$	$f(\epsilon, n)$	$\lambda_{abs}$ (nm)	$\lambda_{em}$ (nm)	$\nu_a$ ( $\text{cm}^{-1}$ )	$\nu_e$ ( $\text{cm}^{-1}$ )	$\nu_a - \nu_e$ ( $\text{cm}^{-1}$ )
Dioxnae	2.25	1.422	0.025	429	509	$2.331 \times 10^4$	$1.965 \times 10^4$	$3.66 \times 10^3$
Ethyl ether	4.34	1.352	0.167	426	506	$2.347 \times 10^4$	$1.976 \times 10^4$	$3.71 \times 10^3$
$\text{CHCl}_3$	4.81	1.446	0.148	425	507	$2.353 \times 10^4$	$1.972 \times 10^4$	$3.81 \times 10^3$
DCM	8.93	1.424	0.217	428	508	$2.336 \times 10^4$	$1.969 \times 10^4$	$3.67 \times 10^3$
Acetone	20.7	1.359	0.284	438	511	$2.283 \times 10^4$	$1.957 \times 10^4$	$3.26 \times 10^3$
EtOH	24.5	1.361	0.289	443	513	$2.257 \times 10^4$	$1.949 \times 10^4$	$3.08 \times 10^3$
MeOH	32.7	1.328	0.309	441	520	$2.268 \times 10^4$	$1.923 \times 10^4$	$3.45 \times 10^3$
ACN	37.5	1.344	0.305	438	513	$2.283 \times 10^4$	$1.949 \times 10^4$	$3.34 \times 10^3$
DMSO	46.7	1.478	0.263	461	528	$2.169 \times 10^4$	$1.894 \times 10^4$	$2.75 \times 10^3$

Table S11. Fluorescence lifetime ( $\tau$ ) of TFEA-Naph, TFEA-Cou and TFEA-NBD in different solvents

Solvent	$\tau$ (ns)		
	TFEA-Naph	TFEA-Cou	TFEA-NBD
Dioxane	9.47	2.66	2.46/6.67
CHCl <sub>3</sub>	8.97	2.75	1.18/8.06
EA	9.08	2.69	4.54/8.33
Acetone	9.43	2.83	9.13
EtOH	10.06	3.35	8.13
MeOH	10.07	3.52	7.68
ACN	9.99	3.00	9.20
DMSO	10.24	3.01	7.80
H <sub>2</sub> O	7.61	4.39	1.40

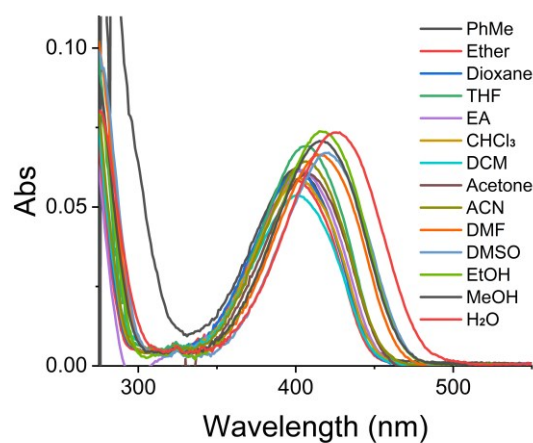


Fig. S1 UV-vis absorption spectra of **TFEA-Naph** (5  $\mu$ M) in different solvents.

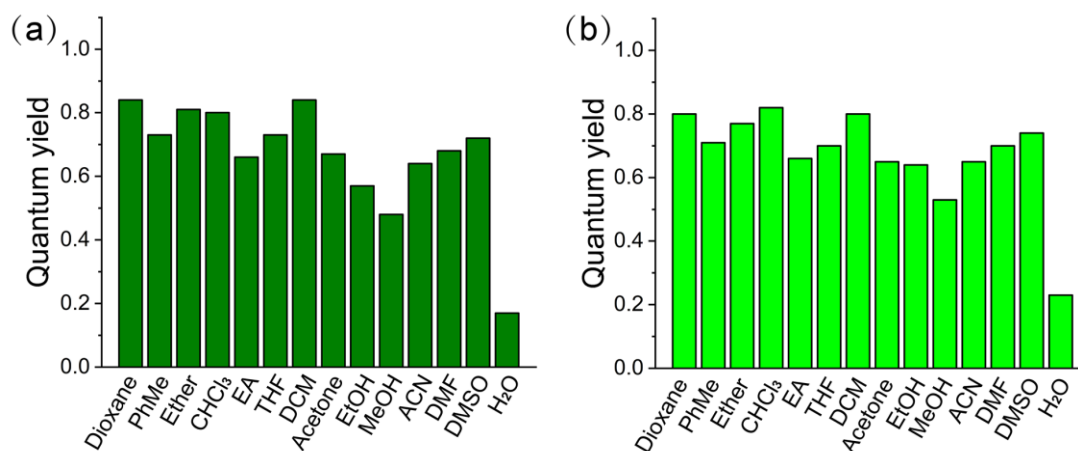


Fig. S2 The fluorescence quantum yields of **EA-Naph** (a) and **Aze-Naph** (b) in different solvents.

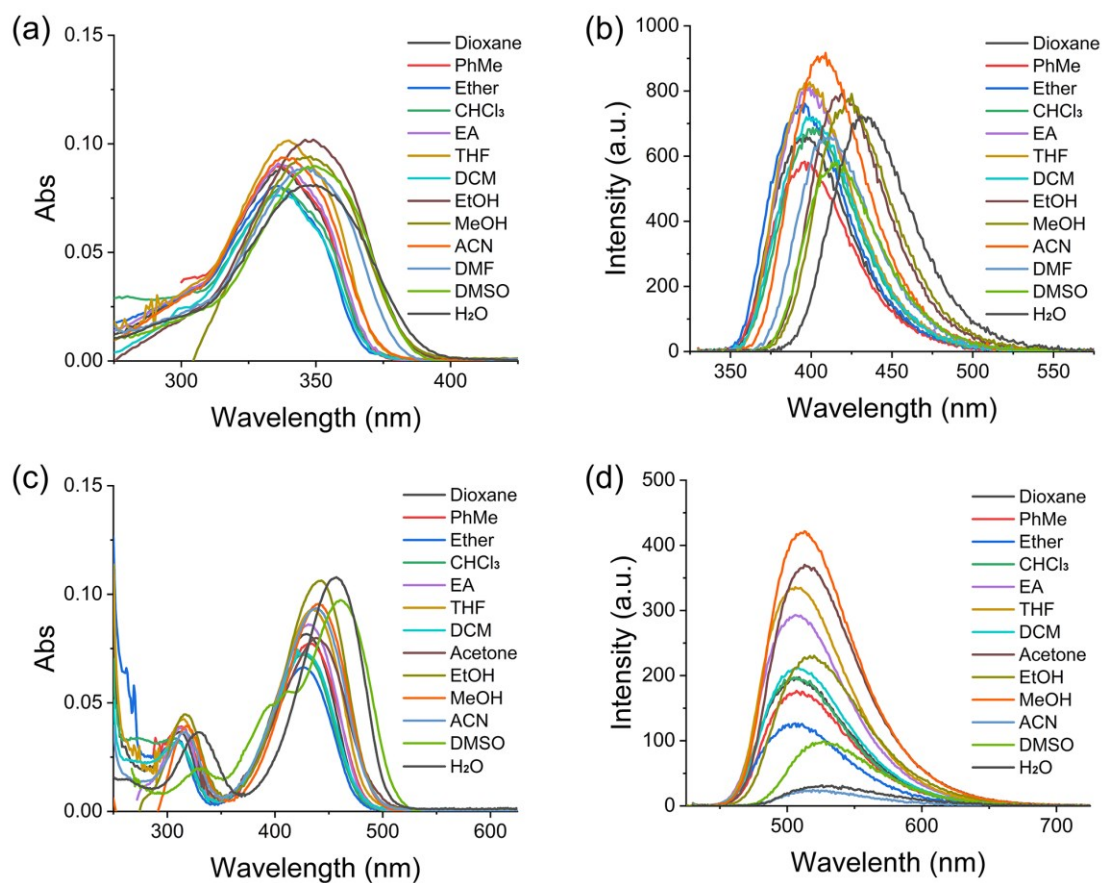
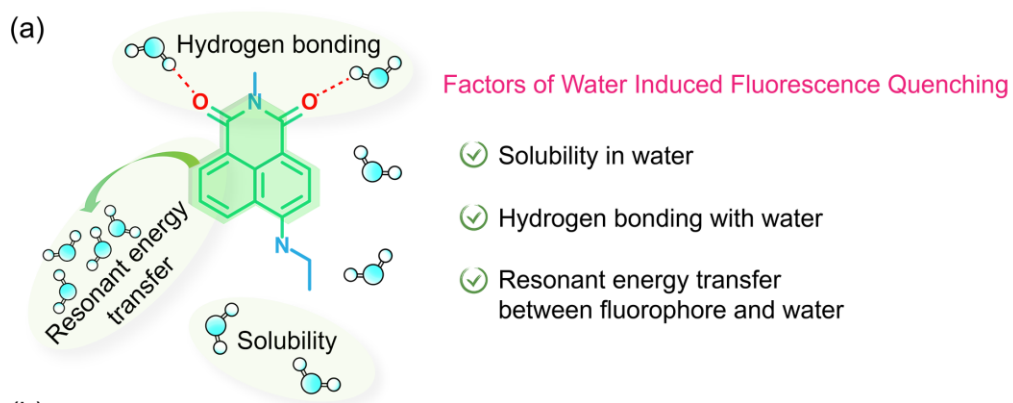


Fig. S3 UV-vis absorption spectra (a) and fluorescence emission spectra (b) of **TFEA-Cou** (5  $\mu\text{M}$ ) in different solvents; UV-vis absorption spectra (c) and fluorescence emission spectra (d) of **TFEA-NBD** (5  $\mu\text{M}$ ) in different solvents.



(b)

Fluorophore	Substituent (R)	Solvent	$\lambda_{\text{abs}}$ (nm)	$\lambda_{\text{em}}$ (nm)	$\Delta\lambda$ (nm)	$\epsilon$ ( $\text{M}^{-1}\text{cm}^{-1}$ )	$\phi$
		H <sub>2</sub> O	426	525	99	14690	0.50
		D <sub>2</sub> O	423	523	100	12600	0.38
	 TFEA-Naph	H <sub>2</sub> O/DMSO (90%/10%)	426	521	95	13760	0.53
		H <sub>2</sub> O/DMSO (50%/50%)	426	514	88	14000	0.78
		H <sub>2</sub> O/DMSO (25%/75%)	422	510	84	13400	0.83
	 TFEA-Naph-1	H <sub>2</sub> O	427	522	95	9400	0.51
		D <sub>2</sub> O	424	525	101	8950	0.38
	 TFEA-Naph-2	H <sub>2</sub> O	426	526	100	11590	0.46
		D <sub>2</sub> O	424	526	102	10430	0.36
	 TFEA-Naph-3	H <sub>2</sub> O	427	521	94	10790	0.50
		D <sub>2</sub> O	424	522	98	10090	0.37

Fig. S4. (a) Factors of water induced fluorescence quenching for naphthalimide dyes; (b) The spectral properties of TFEA-Naph (5  $\mu\text{M}$ ), TFEA-Naph-1 (5  $\mu\text{M}$ ), TFEA-Naph-2 (5  $\mu\text{M}$ ) and TFEA-Naph-3 (5  $\mu\text{M}$ ).



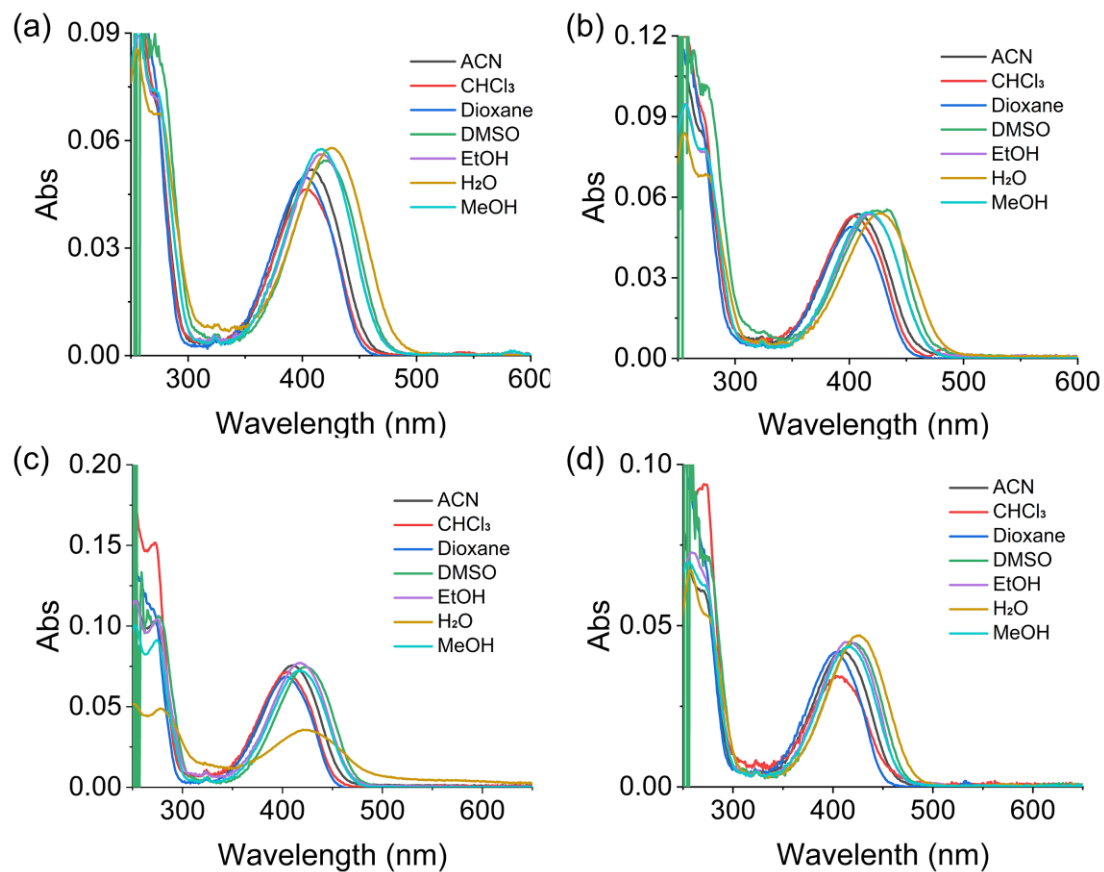


Fig. S5 UV-vis absorption of **TFEA-Naph-2** (5  $\mu$ M) (a), **TFEA-Naph-3** (5  $\mu$ M) (b), **TFEA-Naph-4** (5  $\mu$ M) (c), and **TFEA-Naph-1** (5  $\mu$ M) (d) in different solvents.

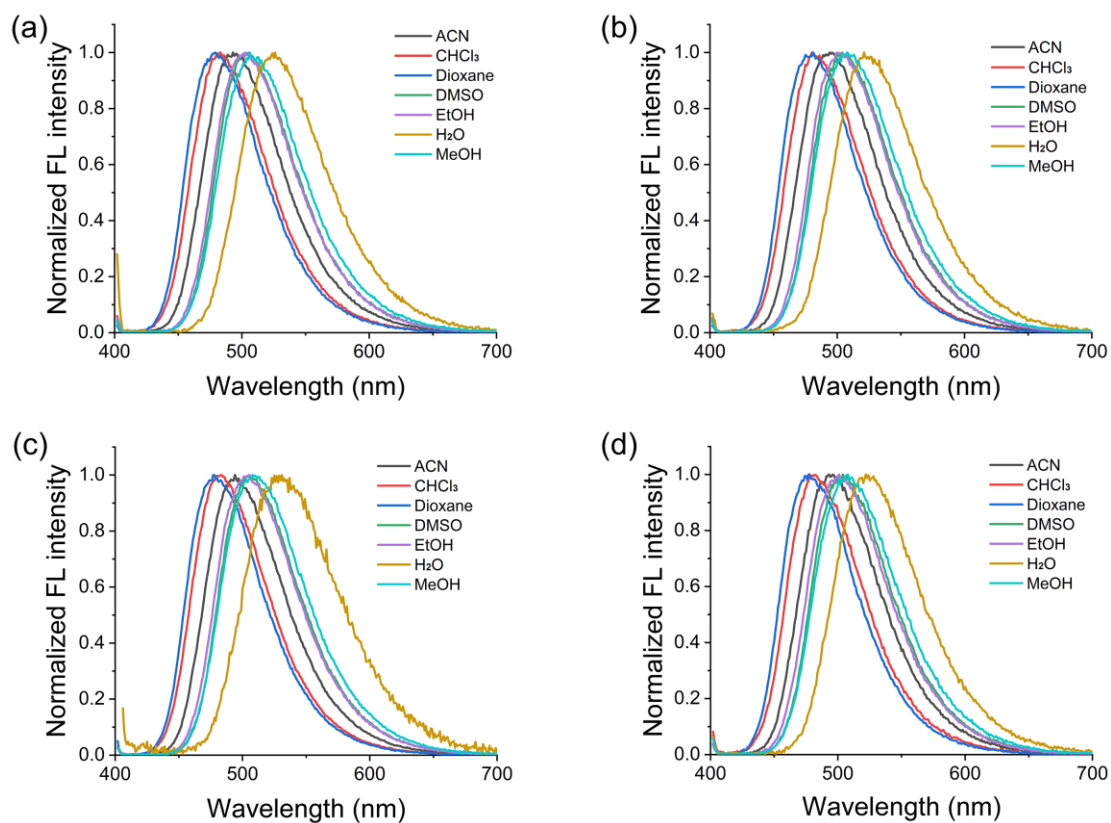


Fig. S6 Normalized fluorescence emission spectra of **TFEA-Naph-2** (5  $\mu$ M,  $\lambda_{ex}$ = 400 nm) (a), **TFEA-Naph-3** (5  $\mu$ M,  $\lambda_{ex}$ = 400 nm) (b), **TFEA-Naph-4** (5  $\mu$ M,  $\lambda_{ex}$ = 400 nm) (c), and **TFEA-Naph-1** (5  $\mu$ M,  $\lambda_{ex}$ = 400 nm) (d) in different solvents.

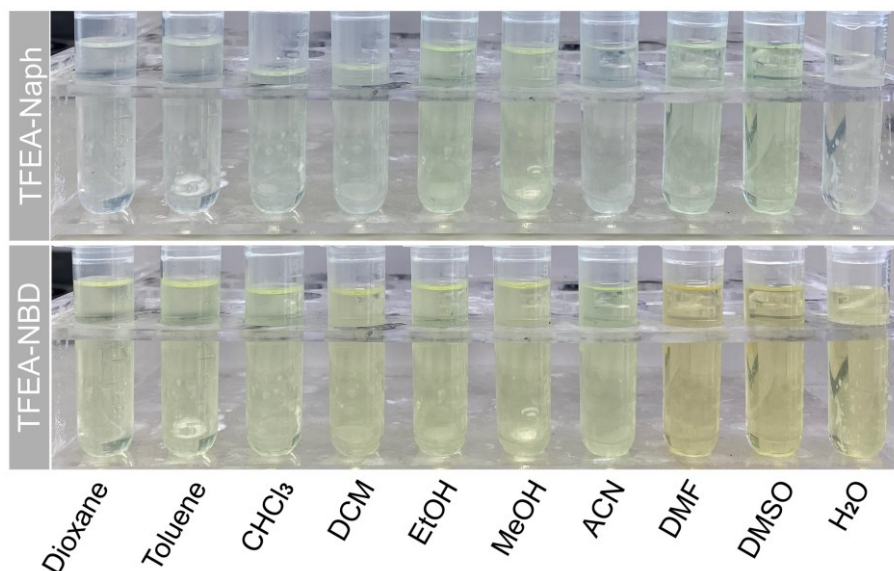


Fig. S7 The image of TFEA-Naph (20 $\mu$ M) (Top) and TFEA-NBD (10 $\mu$ M) (bottom) in different solvents.

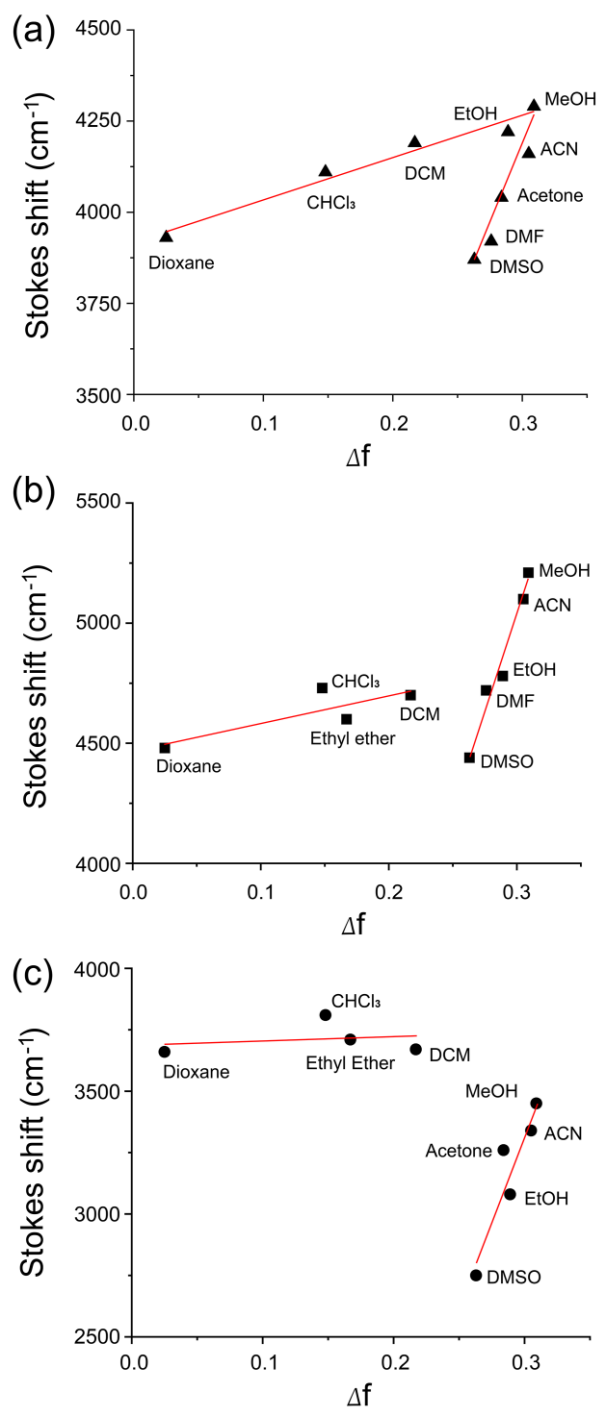


Fig. S8 Lippert–Mataga plot depicting Stokes shift ( $\Delta\nu$ ) versus the solvent orientation polarizability ( $\Delta f$ ) of TFEA-Naph (a), TFEA-Cou (b) and TFEA-NBD (c).

## 4 Imaging details

We examined the performance of **TFEA-Naph**, **TFEA-Cou** and **TFEA-NBD** in living cells. First, HeLa cells were incubated with **TFEA-Naph** for 45 minutes before imaging. Owing to the electron-withdrawing trifluoroethylamine group causing a blue-shift in the absorption and emission wavelength, the initial imaging channel was set to collect from 425-525 nm for imaging. As shown in Fig. S9a, the fluorescence of **TFEA-Naph** was distributed in the cytoplasm and lipid droplets of the cells. Considering the difference in polarity between the lipophilic environment of lipid droplets and the polar environment of the cytoplasm, as well as the polarity-sensitive property of **TFEA-Naph**, we attempted to selectively visualize the distribution of **TFEA-Naph** in cells by adjusting the collection channel range. As expected, when we blue-shifted the collection channel and narrowed the collection range, the fluorescence of **TFEA-Naph** was distinctly observed only in lipid droplets, with a background fluorescence signal-to-noise ratio of only 3.4. By expanding the range of collection channel to 100 nm, the fluorescence of **TFEA-Naph** distributed in the highly polar region (cytoplasm) could be observed, and the signal-to-noise ratio of cytoplasmic background fluorescence reached 12.8. As we further red-shifted the collection channel to 500-600 nm, the fluorescence in lipid droplets weakened while that in the cytoplasm continued to increase (signal-to-noise ratio 15.5). Analysis of the fluorescence intensity in the cytoplasm and extracellular region also verified this finding (Fig. S9b). Since the absorption wavelength of **TFEA-Cou** was below 400 nm, the common 405 nm excitation light source could not image. We attempted to observe its distribution in cells with the help of two-photon excitation microscopy. Considering the weak two-photon absorption capability of **TFEA-Cou**, we increased the concentration of the probe during staining. As shown in Fig. S9c, **TFEA-Cou** exhibited no distinct targeting in cells regardless of the probe concentration. Similarly, confocal imaging of **TFEA-NBD** in HeLa cells also showed no specific distribution (Fig. S9d). We believe that the introduction of specific targeting groups into **TFEA-NBD** and **TFEA-Cou** will expand their applications in the field of cell imaging in the future.

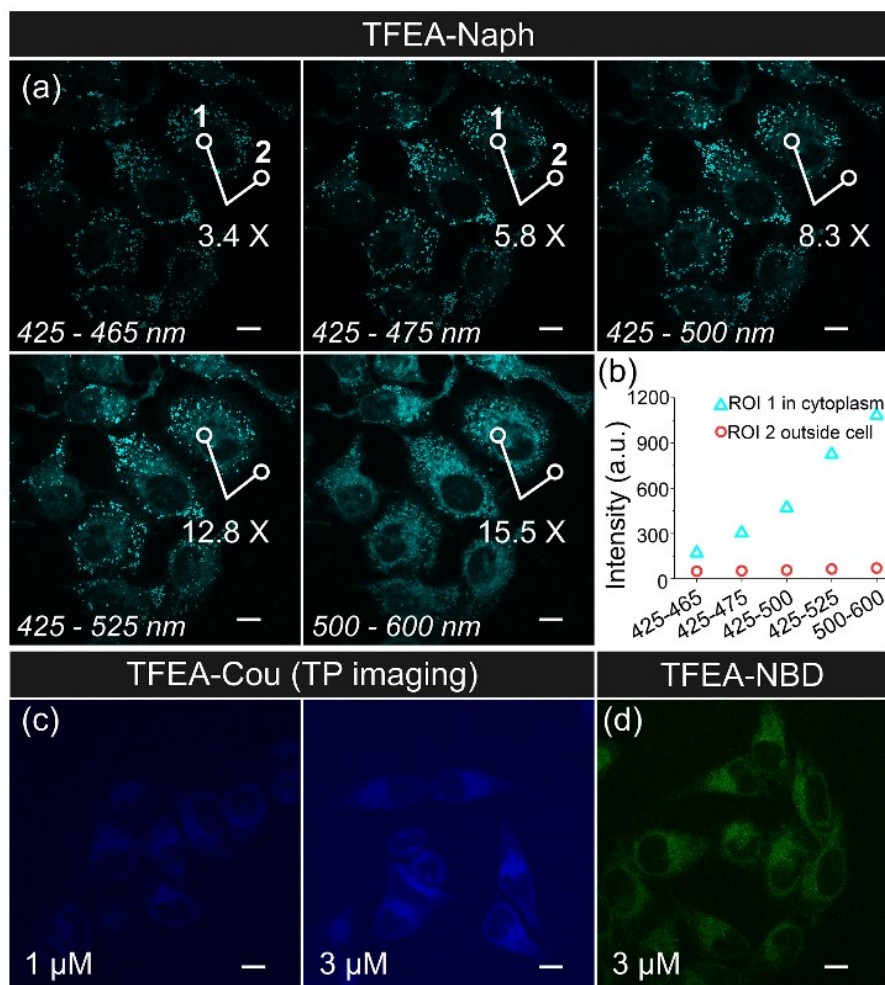


Fig. S9 (a) Confocal imaging lipid droplets under different collection channels using **TFEA-Naph** (500nM); (b) Ratio of cytoplasmic and extracellular fluorescence intensity under different collection channels; (c) Two-photon imaging (770nm) of **TFEA-Cou** at 1  $\mu$ M or 3  $\mu$ M in HeLa cells; (d) Confocal imaging of **TFEA-NBD** at 3  $\mu$ M in HeLa cells. Scale bar = 10  $\mu$ m.

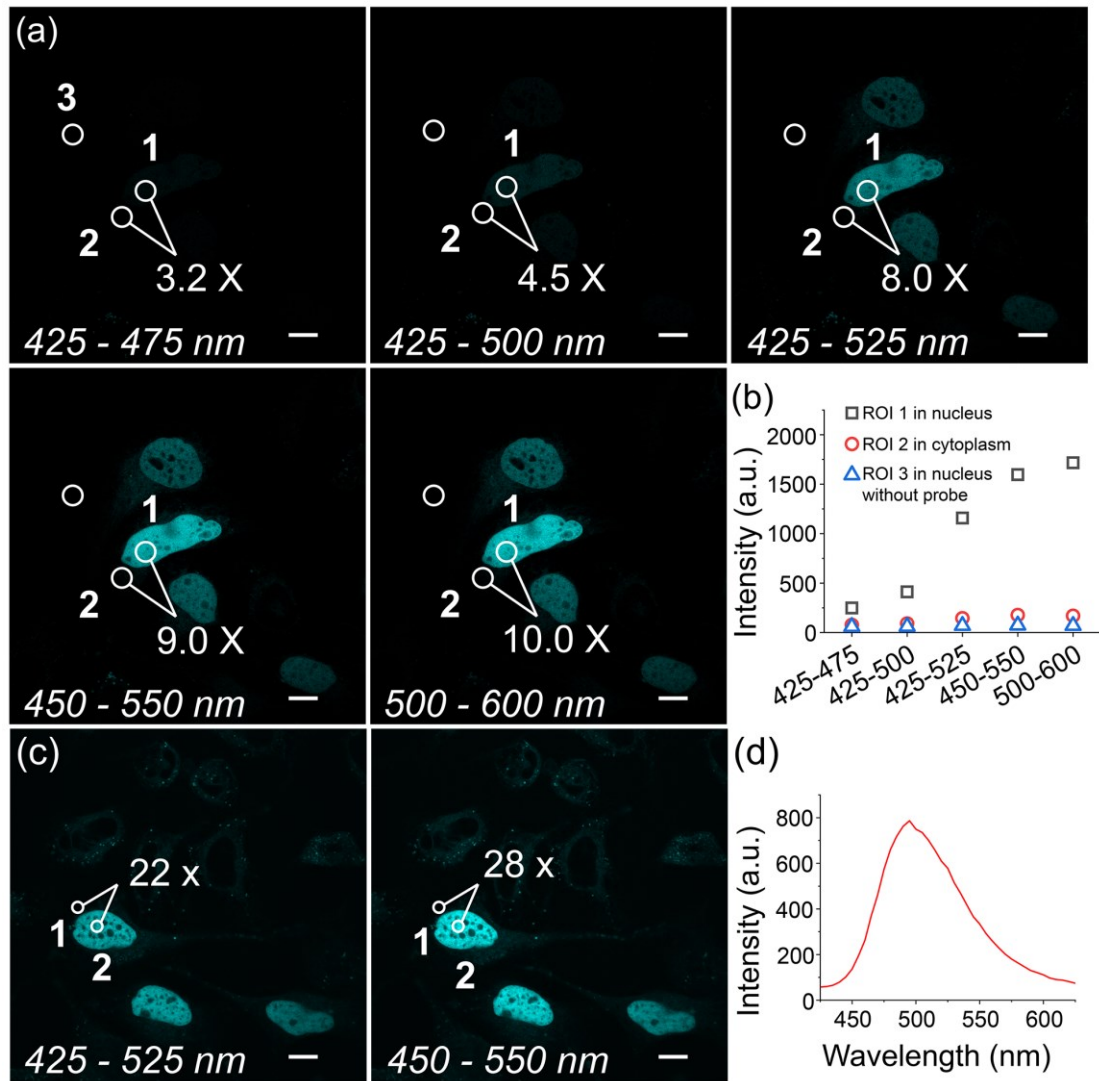


Fig. S10 (a) Confocal imaging of nucleus in HeLa cells transfected with Halo-H2B plasmid under different collection channels using **TFEA-Naph-Halo** (500 nM) and ratio of fluorescence intensity in the nucleus and cytoplasm; (b) The fluorescence intensity in region of interest 1, 2 and 3 in (a); (c) Confocal imaging of nucleus in HeLa cells transfected with Halo-H2B plasmid under different collection channels using **TFEA-Naph-Halo** (500 nM); (d) In-situ spectroscopy of **TFEA-Naph-Halo** labelling nucleus in (c). Scale bar: 10  $\mu$ m.

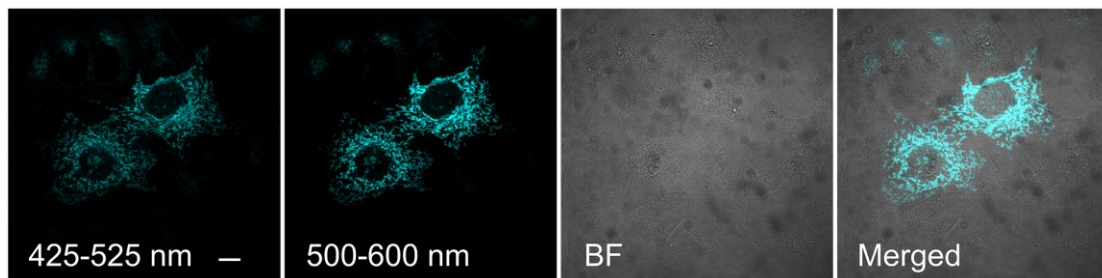


Fig. S11 Confocal imaging of mitochondria in HeLa cells transfected with Halo-Tommon20 plasmid under different collection channels using **TFEA-Naph-Halo** (300 nM). Scale bar: 10  $\mu$ m.

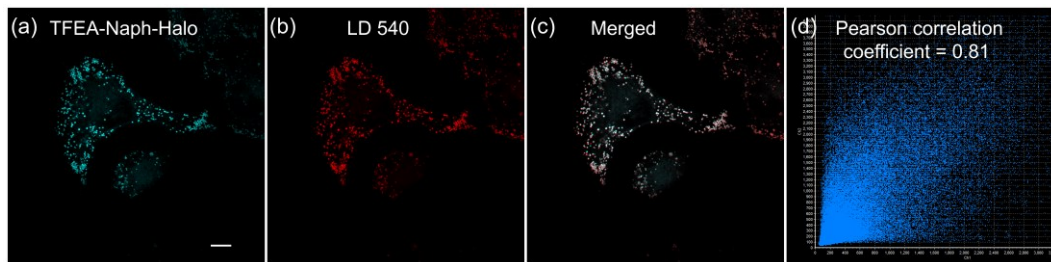


Fig. S12 No-wash confocal imaging of **TFEA-Naph-Halo** (a), commercial dye LD 540 (b); Overlay image of **TFEA-Naph-Halo** and LD 540 (c) and colocalization analysis with Pearson correlation coefficient (d) in HeLa cells at 500 nM. Scale bar: 10  $\mu$ m.

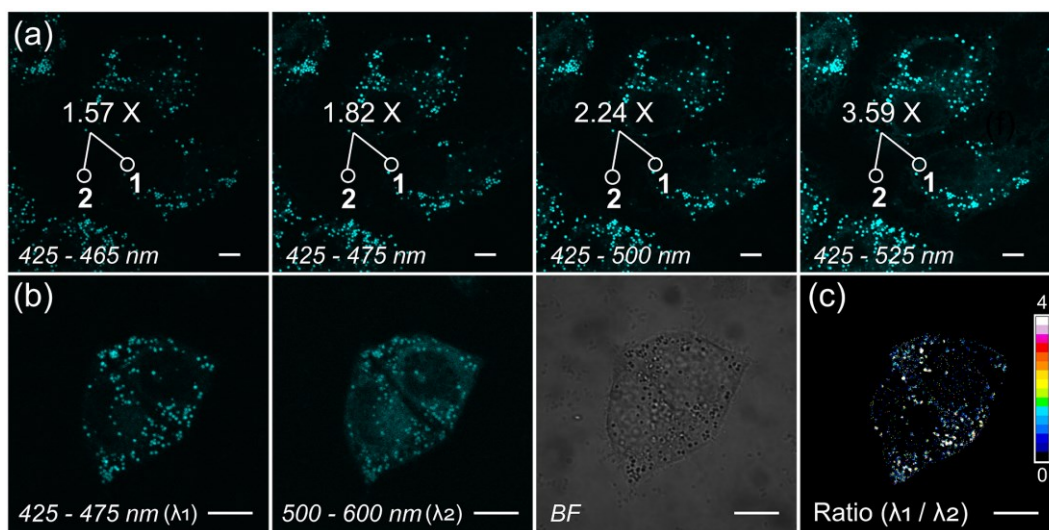


Fig. S13 (a) Confocal imaging of lipid droplets in HeLa cells not transfected with Halo-H2B plasmid under different collection channels using **TFEA-Naph-Halo** (500 nM); (b) Confocal imaging of lipid droplets in HeLa cells under different collection channels using **TFEA-Naph-Halo** (500 nM); (c) Ratio fluorescence plot of **TFEA-Naph-Halo** (500 nM) by a dual-emission channel ( $\lambda_1 = 425-475$  nm;  $\lambda_2 = 500-600$  nm; ratio =  $\lambda_1 / \lambda_2$ ) at  $\lambda_{ex} = 405$  nm in HeLa cells. Scale bar: 10  $\mu$ m.

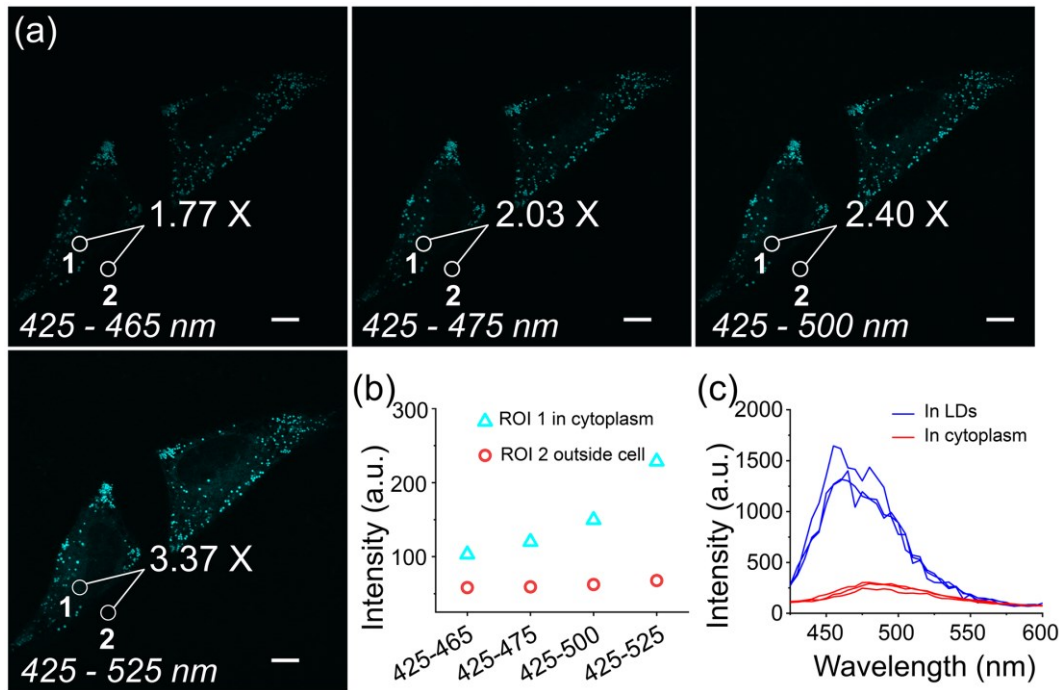


Fig. S14 (a) Confocal imaging of lipid droplets in HeLa cells under different collection channels using **TFEA-Naph-Halo** (500 nM) and ratio of fluorescence intensity in the cytoplasm and outside the cell; (b) The fluorescence intensity in region of interest 1 and 2 in (a); (c) In-situ spectroscopy of **TFEA-Naph-Halo** in lipid droplets and cytoplasm labelling nucleus in (a). Scale bar = 10  $\mu\text{m}$ .

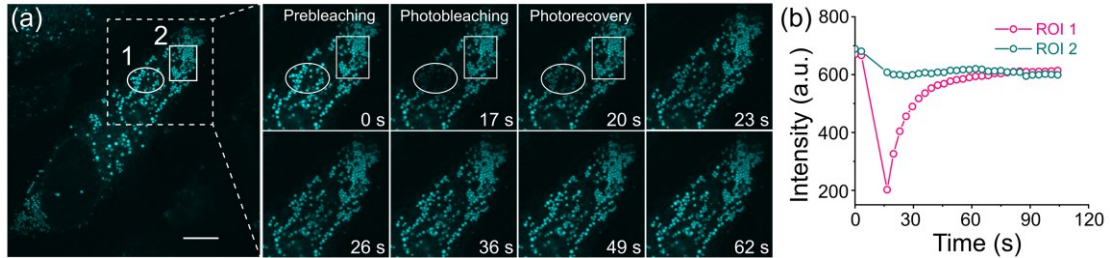


Fig. S15 Confocal images of 0.5  $\mu\text{M}$  **TFEA-Naph-Halo** in living HeLa cells during photobleaching and photorecovery processes. White circle highlighted the bleaching area. (b) Relative intensity of the white circle in bleaching area during photobleaching and photorecovery processes in (a). Scale bar = 10  $\mu\text{m}$ .



## 5 Spectra characterization

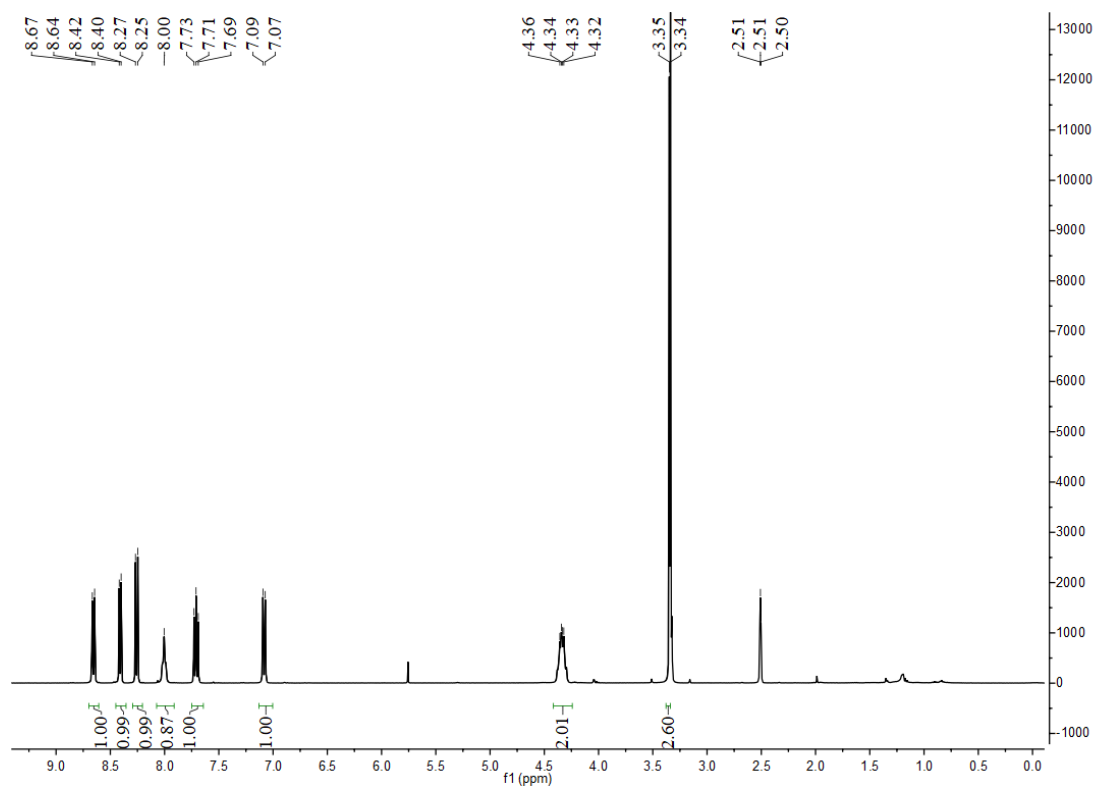


Fig. S16 <sup>1</sup>H NMR spectrum of TFEA-Naph in DMSO-*d*<sub>6</sub>.

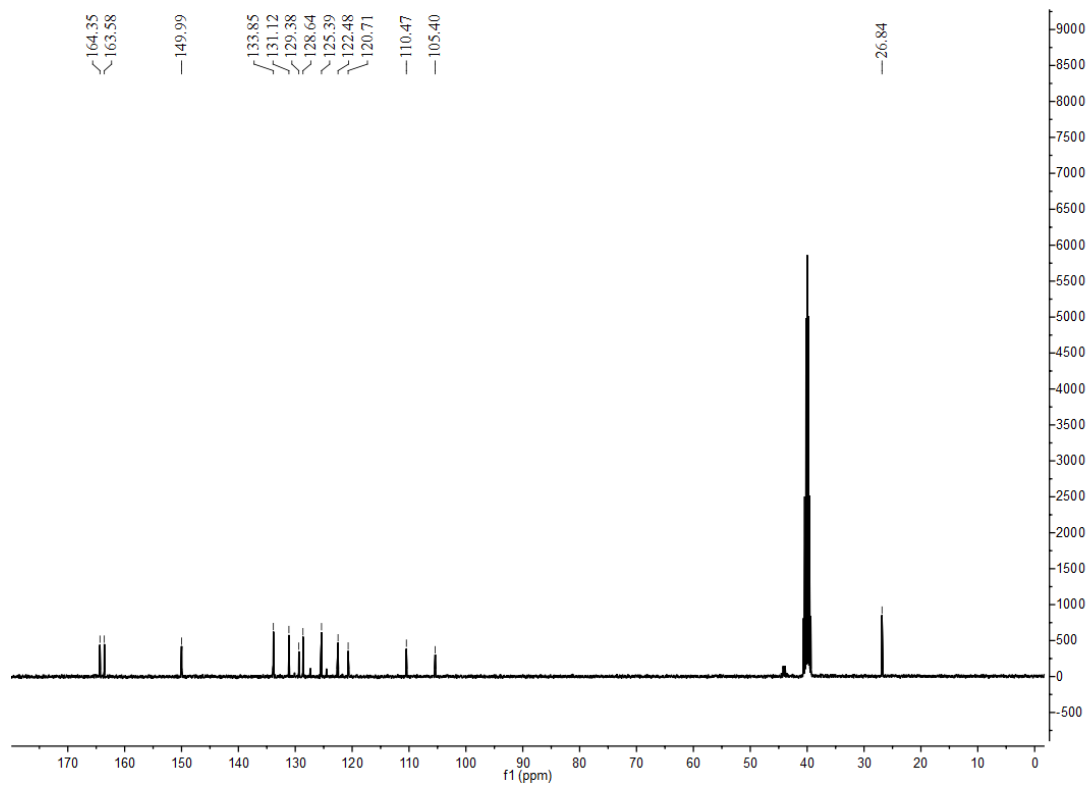


Fig. S17 <sup>13</sup>C NMR spectrum of TFEA-Naph in DMSO-*d*<sub>6</sub>.

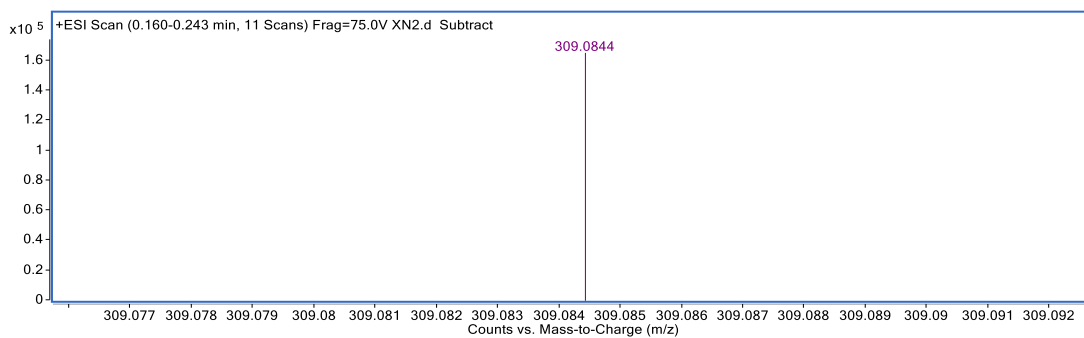


Fig. S18 HRMS spectrum of TFEA-Naph.

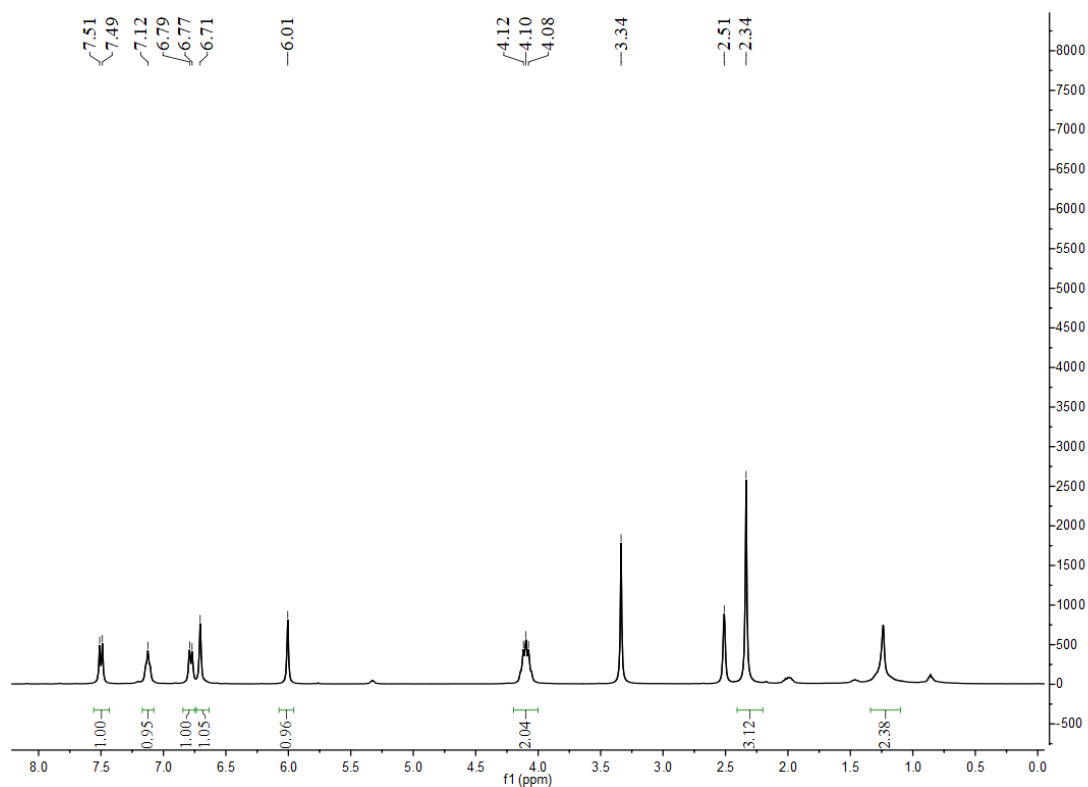


Fig. S19 <sup>1</sup>H NMR spectrum of TFEA-Cou in DMSO-d<sub>6</sub>.

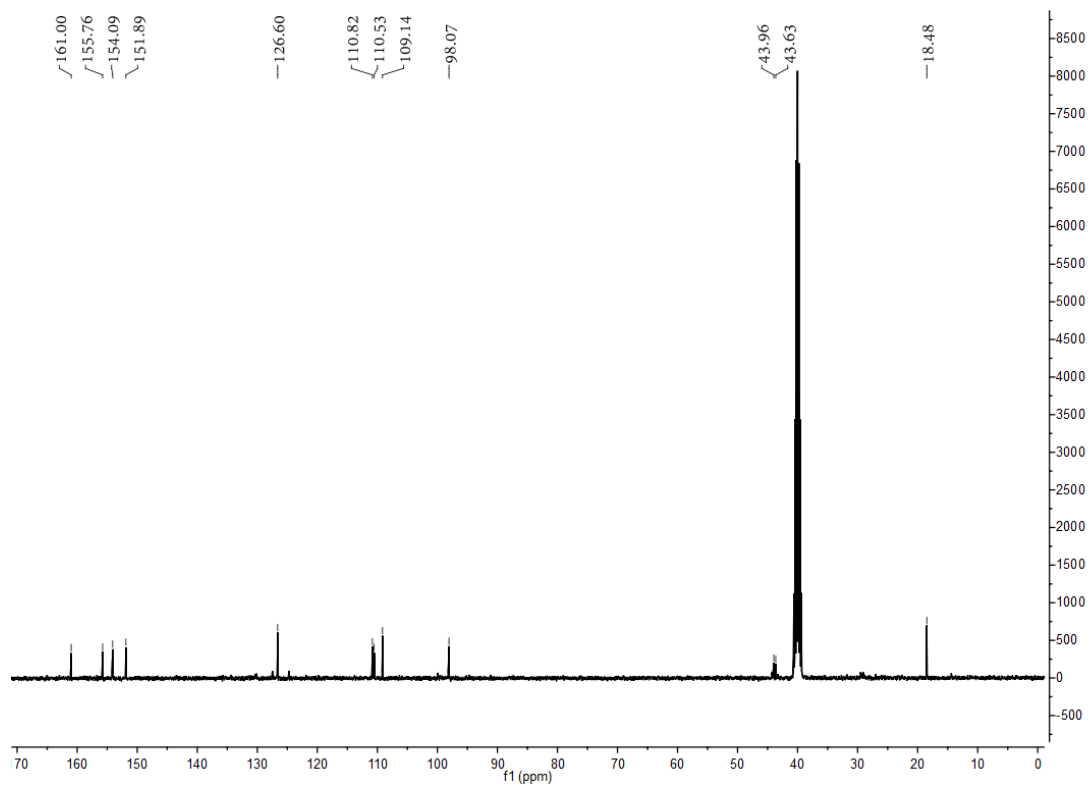


Fig. S20  $^{13}\text{C}$  NMR spectrum of TFEA-Cou in  $\text{DMSO-}d_6$ .

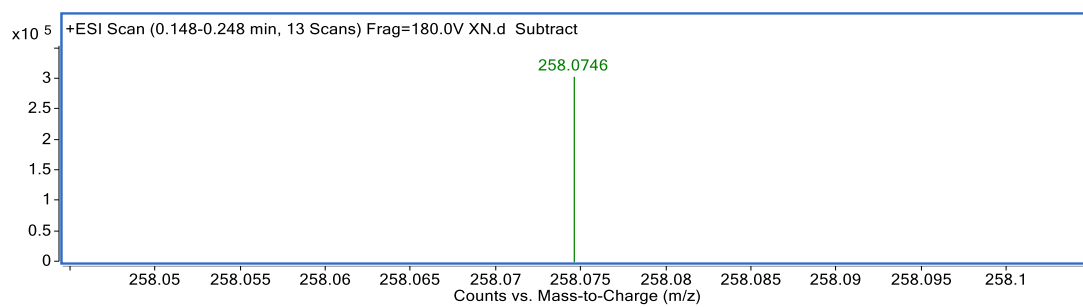


Fig. S21 HRMS spectrum of TFEA-Cou.

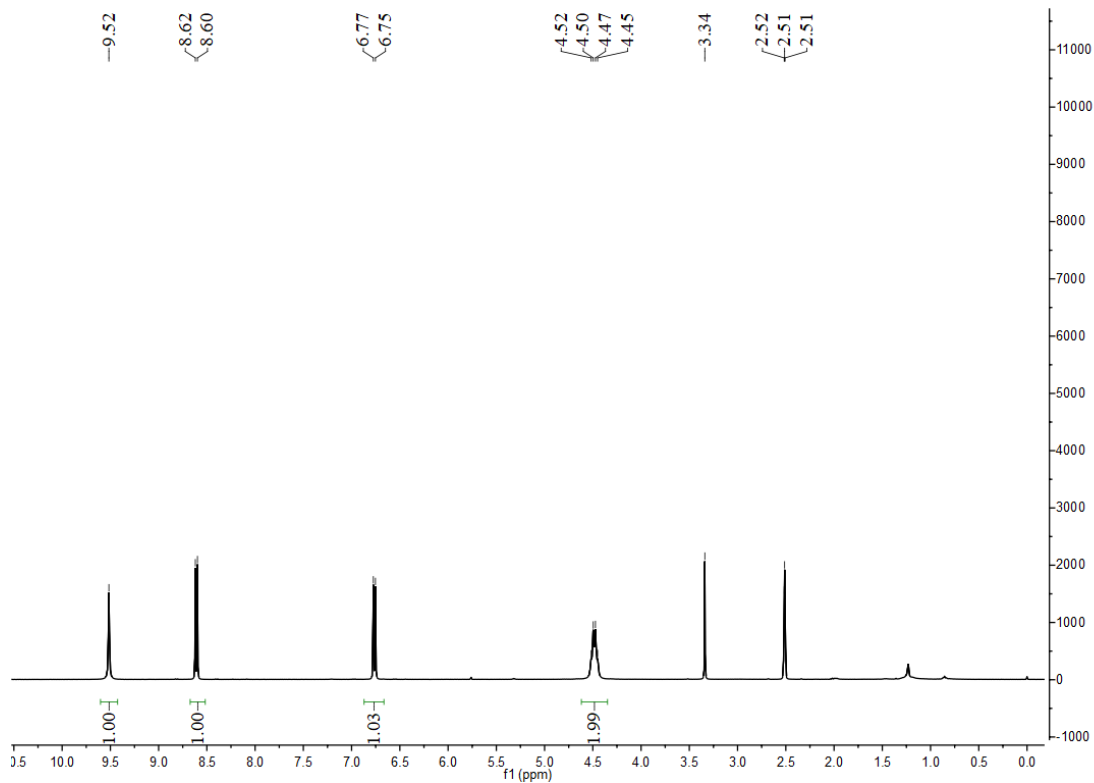


Fig. S22  $^1\text{H}$  NMR spectrum of L TFEA-NBD in  $\text{DMSO-}d_6$ .

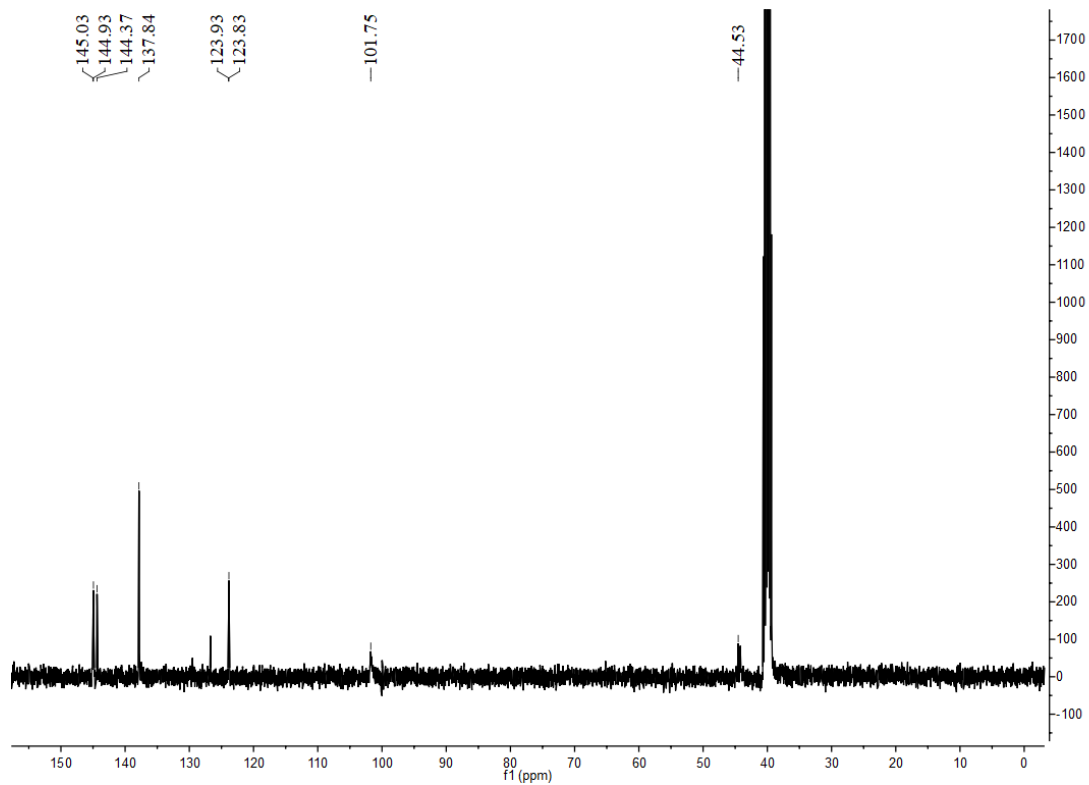


Fig. S23  $^{13}\text{C}$  NMR spectrum of TFEA-NBD in  $\text{DMSO-}d_6$ .

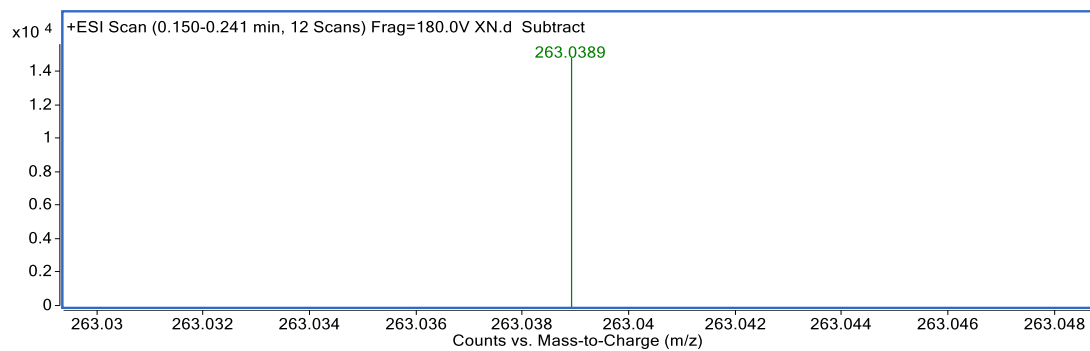


Fig. S24 HRMS spectrum of TFEA-NBD.

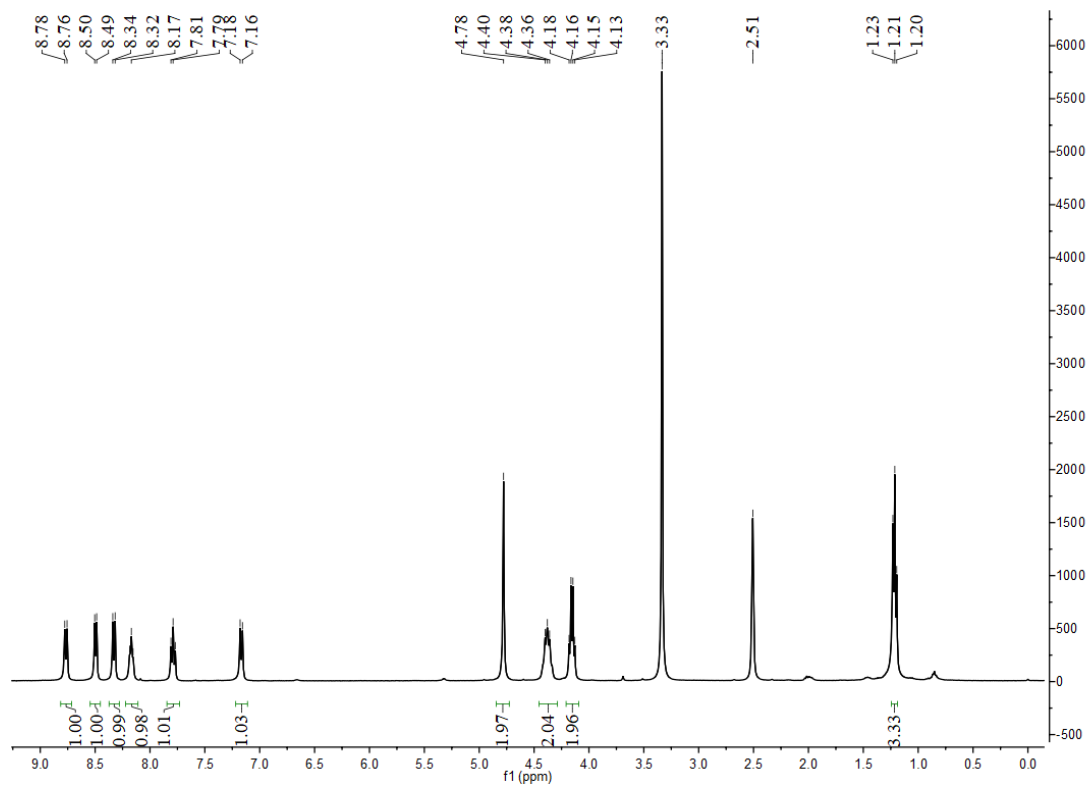


Fig. S25 <sup>1</sup>H NMR spectrum of TFEA-Naph-4 in DMSO-d<sub>6</sub>.

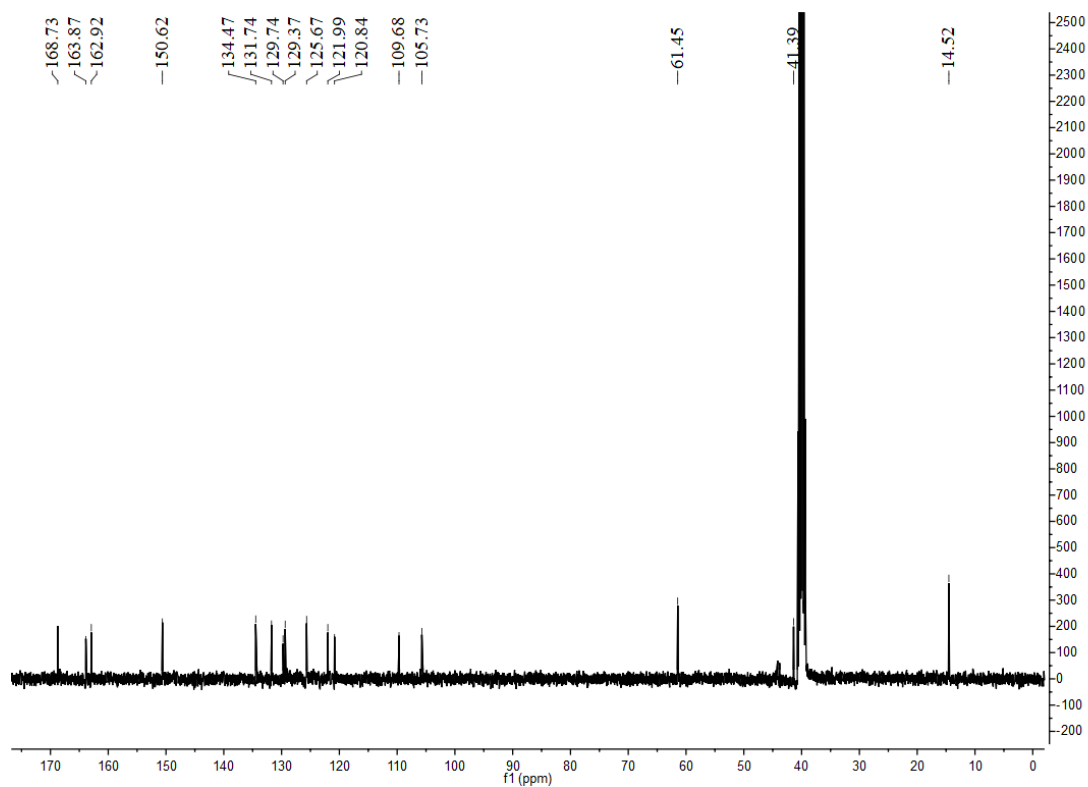


Fig. S26  $^{13}\text{C}$  NMR spectrum of TFEA-Naph-4 in  $\text{DMSO-}d_6$ .

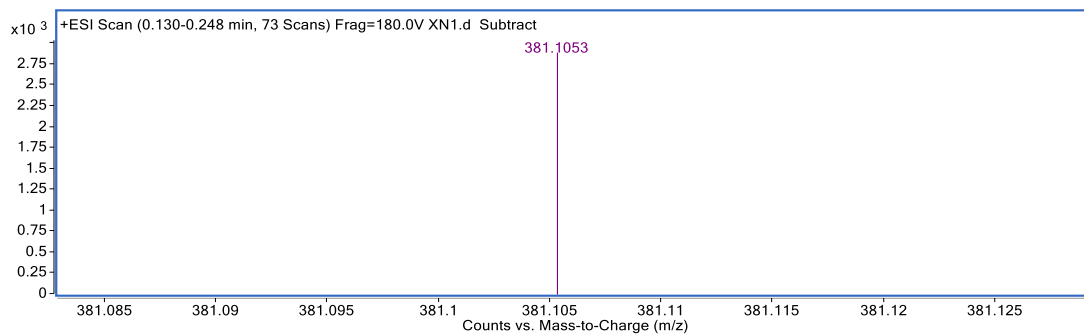


Fig. S27 HRMS spectrum of TFEA-Naph-4.

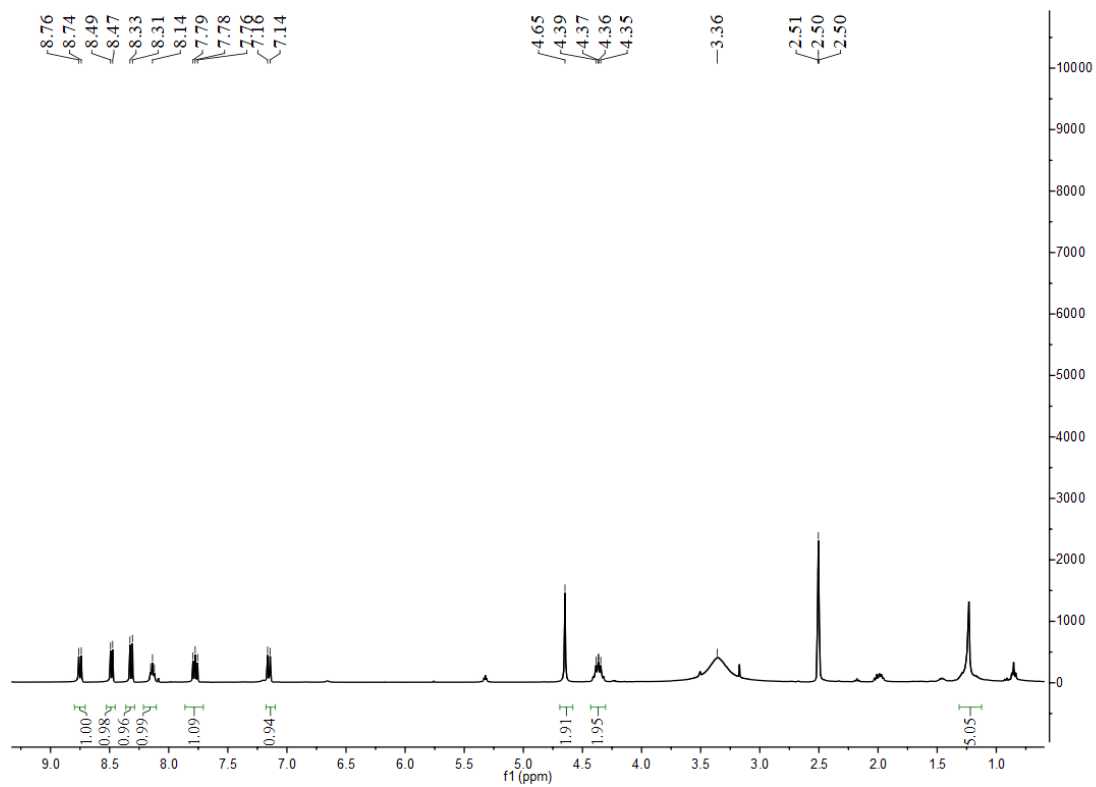


Fig. S28  $^1\text{H}$  NMR spectrum of TFEA-Naph-1 in  $\text{DMSO-}d_6$ .

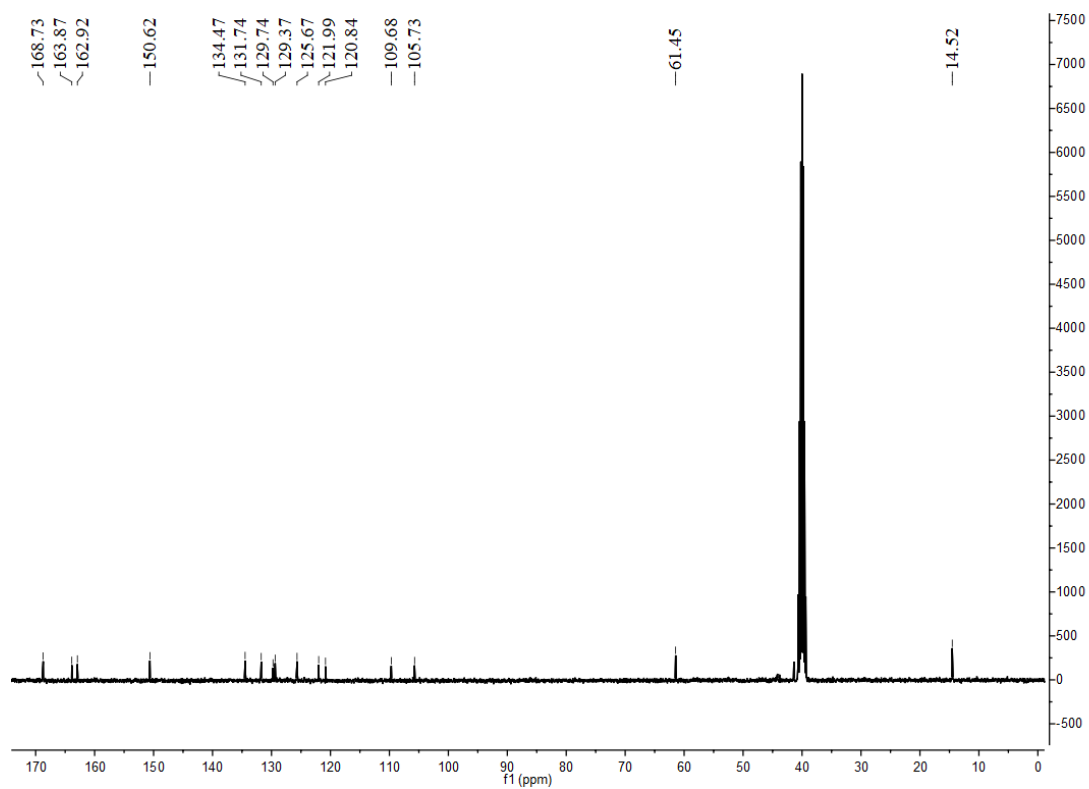


Fig. S29  $^{13}\text{C}$  NMR spectrum of TFEA-Naph-1 in  $\text{DMSO-}d_6$ .

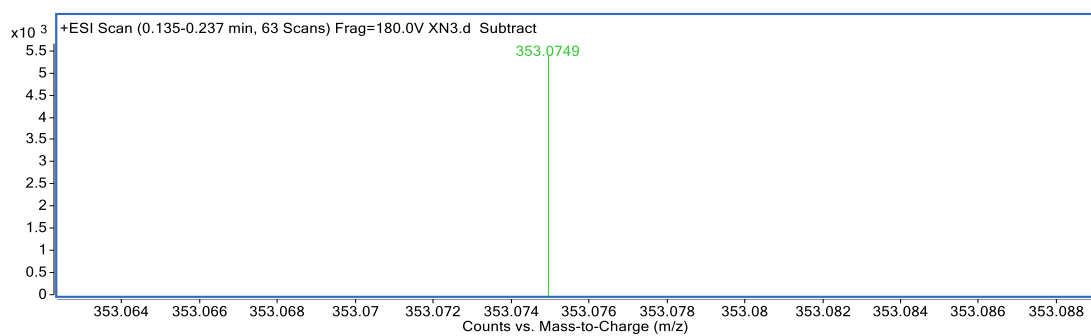


Fig. S30 HRMS spectrum of **TFEA-Naph-1**.

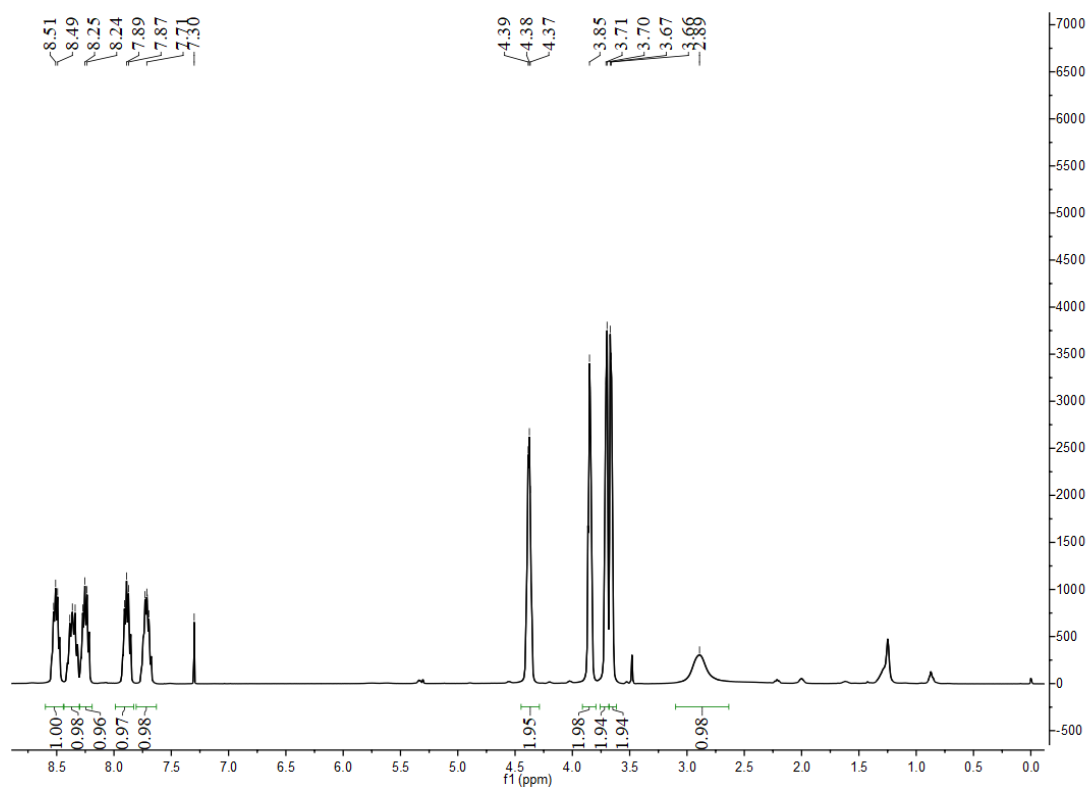


Fig. S31 <sup>1</sup>H NMR spectrum of **Br-Naph-2** in CHCl<sub>3</sub>.



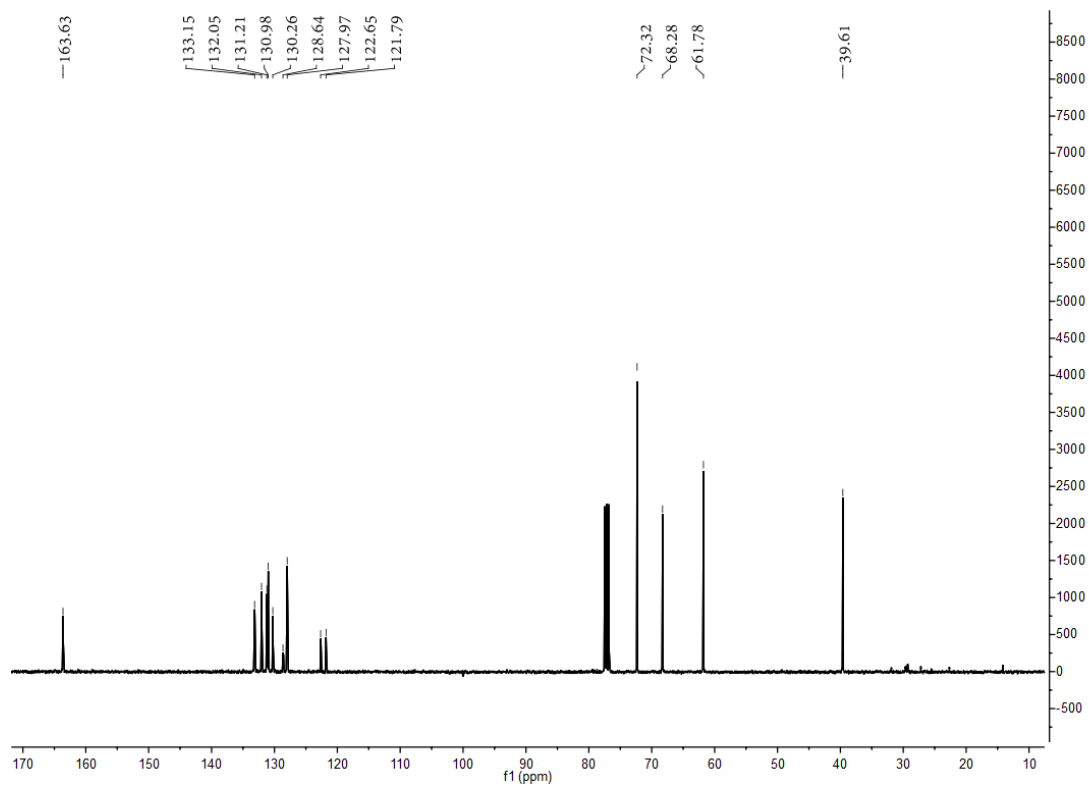


Fig. S32 <sup>13</sup>C NMR spectrum of **Br-Naph-2** in CHCl<sub>3</sub>.

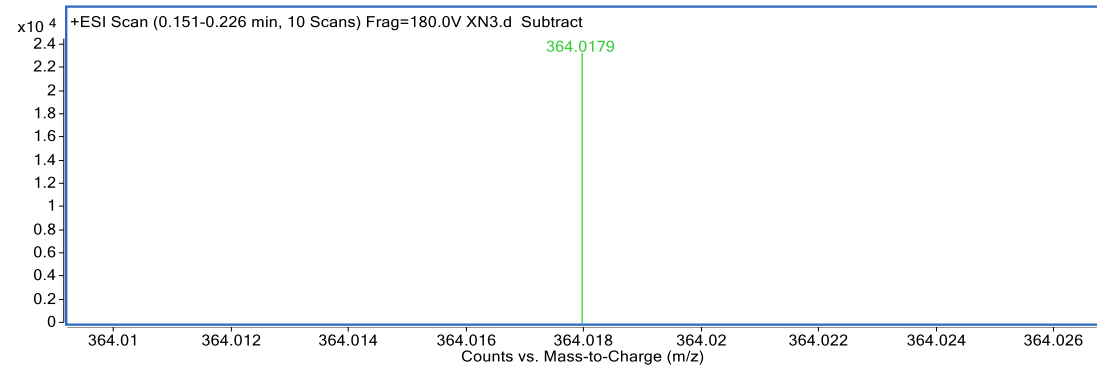


Fig. S33 HRMS spectrum of **Br-Naph-2**.

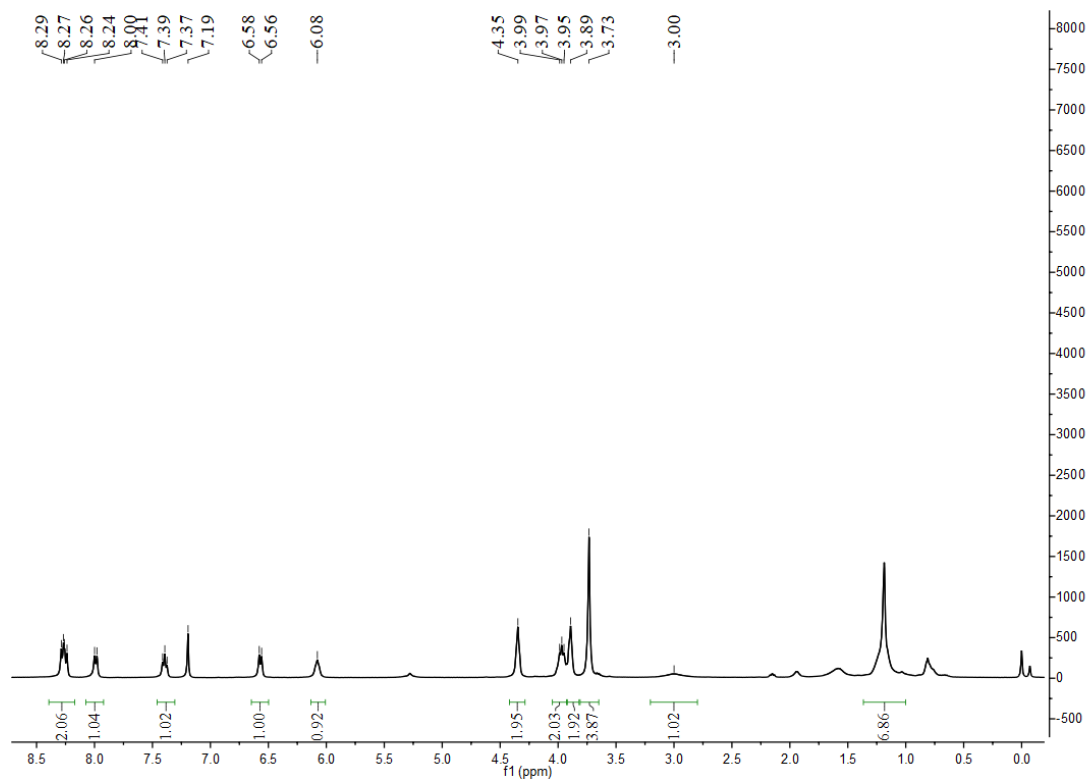


Fig. S34  $^1\text{H}$  NMR spectrum of TFEA-Naph-2 in  $\text{CDCl}_3$ .

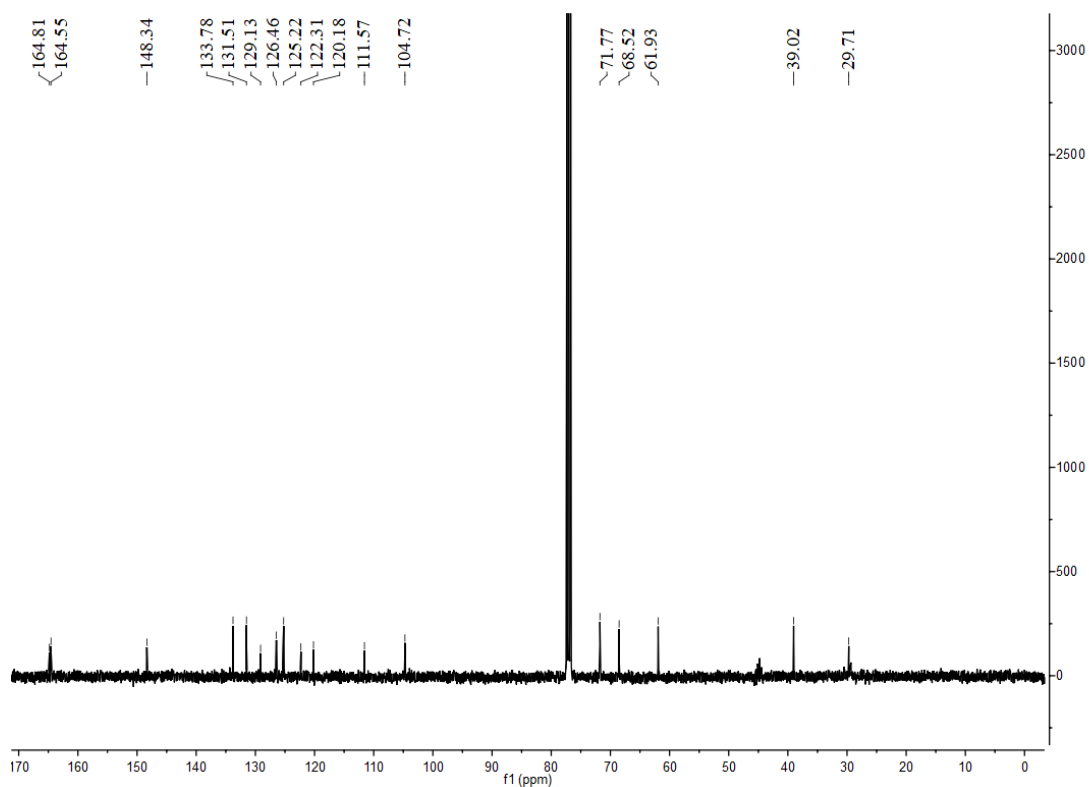


Fig. S35  $^{13}\text{C}$  NMR spectrum of TFEA-Naph-2 in  $\text{CDCl}_3$ .

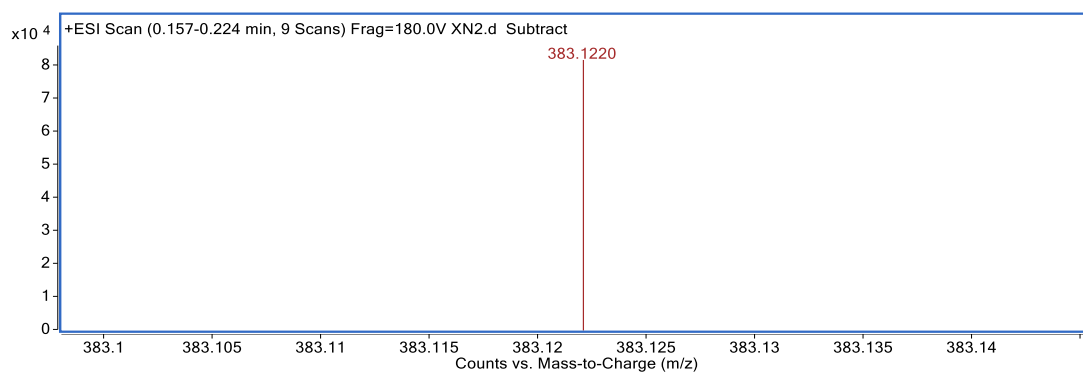


Fig. S36 HRMS spectrum of **TFEA-Naph-2**.

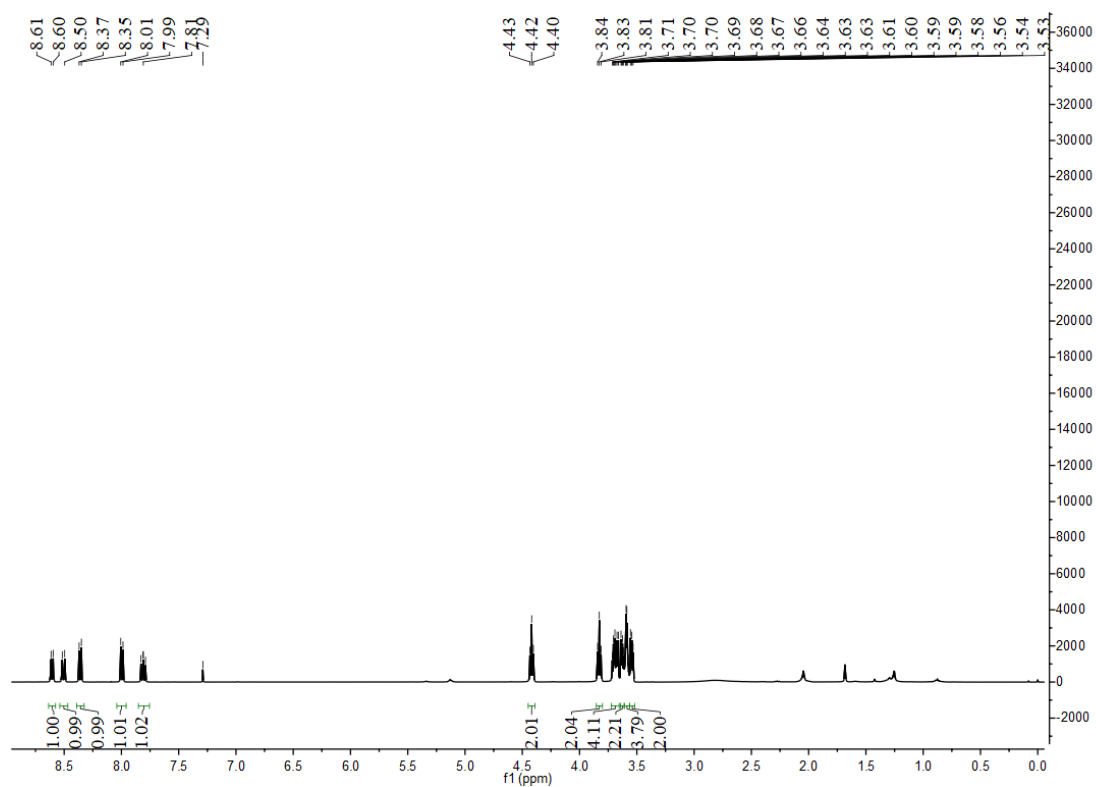


Fig. S37  $^1\text{H}$  NMR spectrum of **Br-Naph-3** in  $\text{CDCl}_3$ .

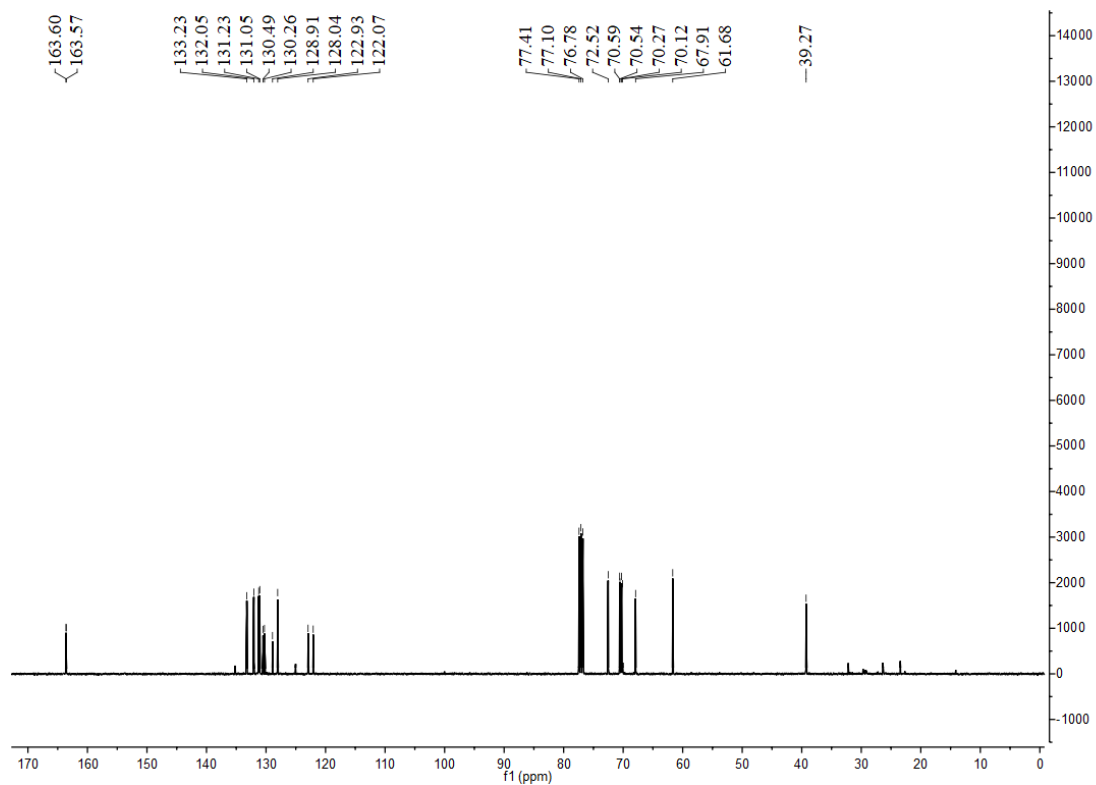


Fig. S38  $^{13}\text{C}$  NMR spectrum of **Br-Naph-3** in  $\text{CDCl}_3$ .

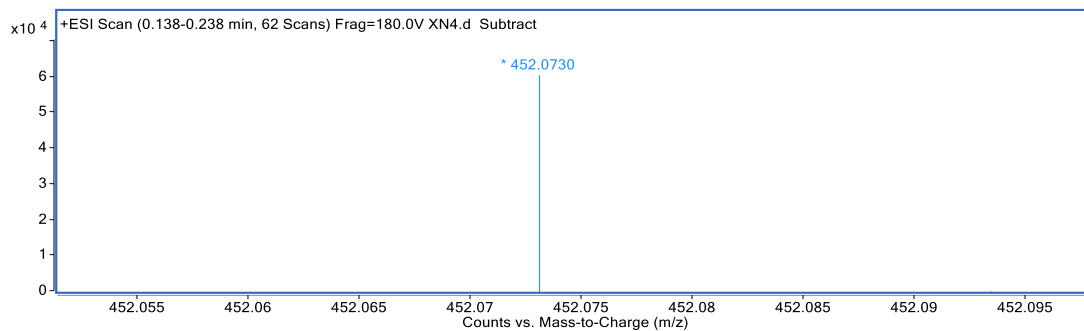


Fig. S39 HRMS spectrum of **Br-Naph-3**.

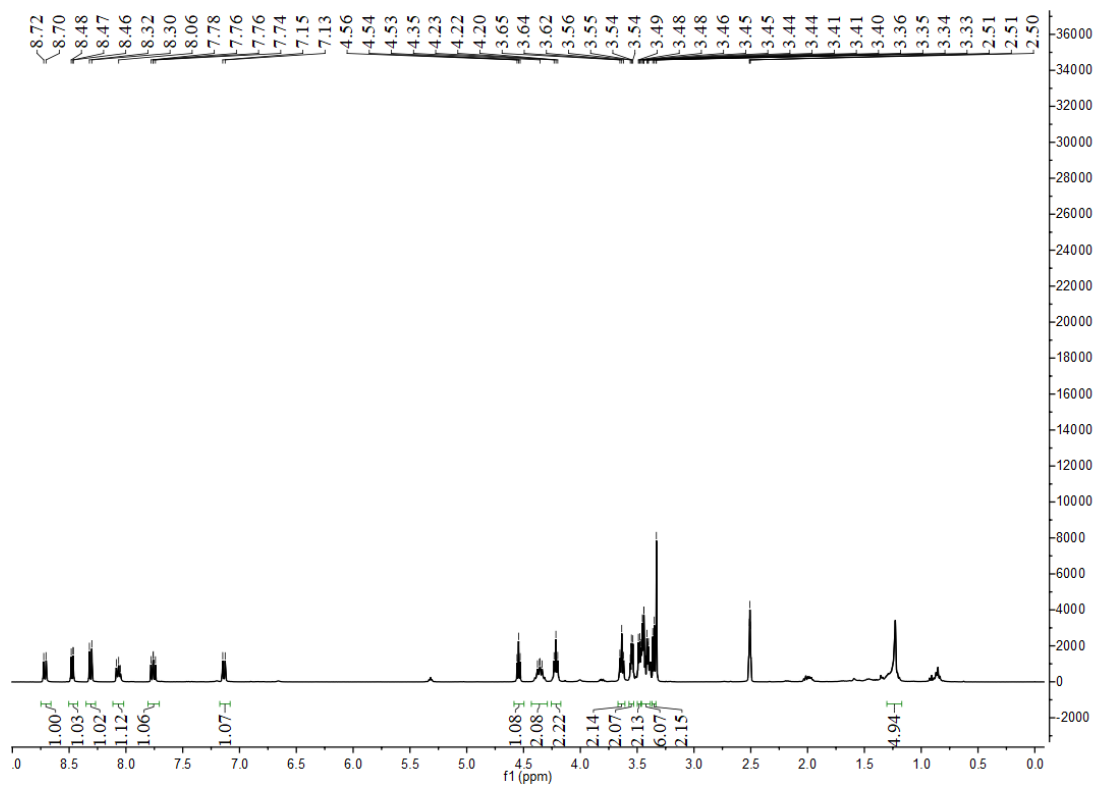


Fig. S40  $^1\text{H}$  NMR spectrum of TFEA-Naph-3 in  $\text{DMSO-}d_6$ .

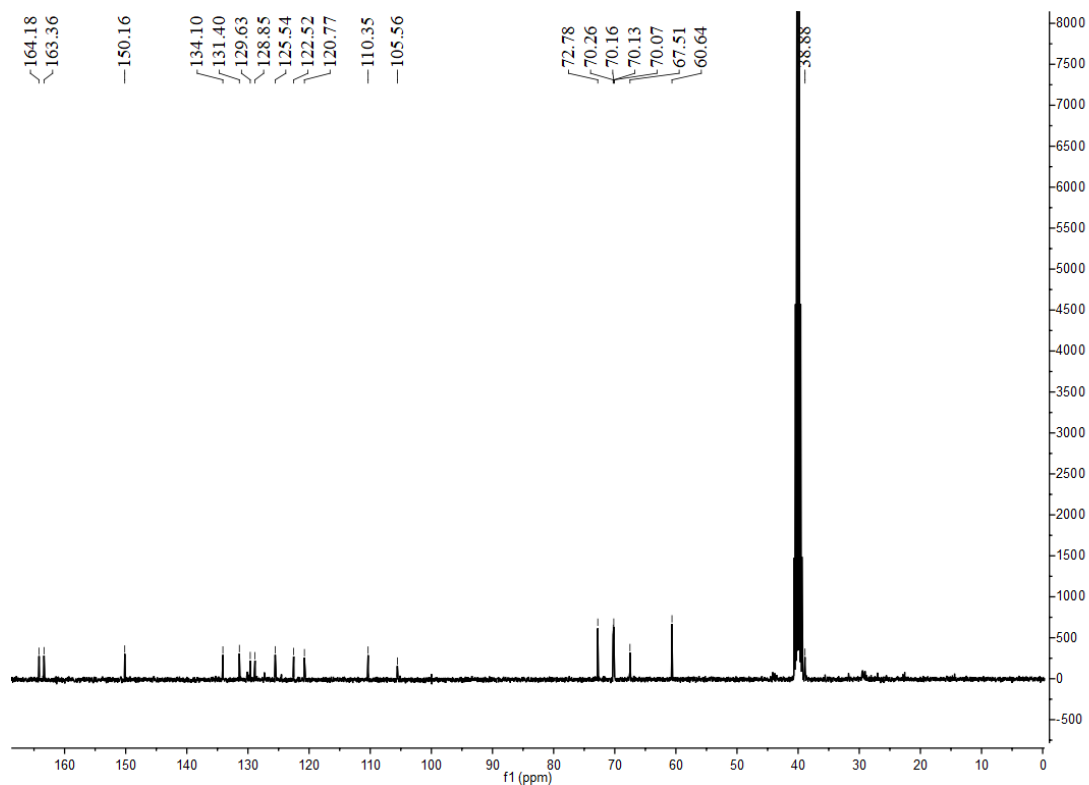


Fig. S41  $^{13}\text{C}$  NMR spectrum of TFEA-Naph-3 in  $\text{DMSO-}d_6$ .

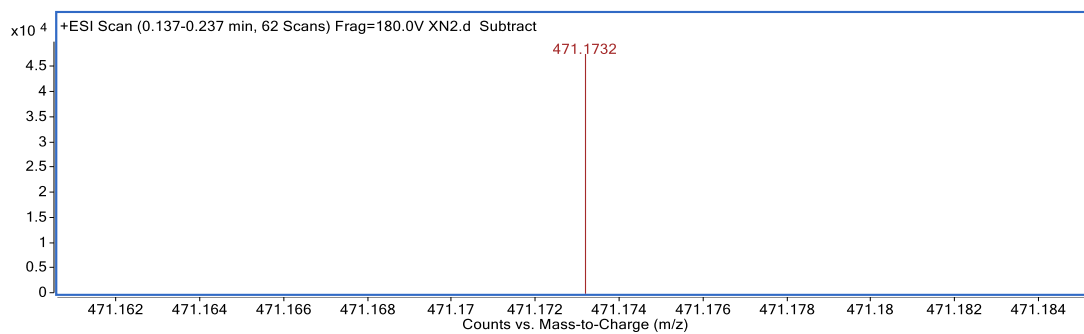


Fig. S42 HRMS spectrum of TFEA-Naph-3.

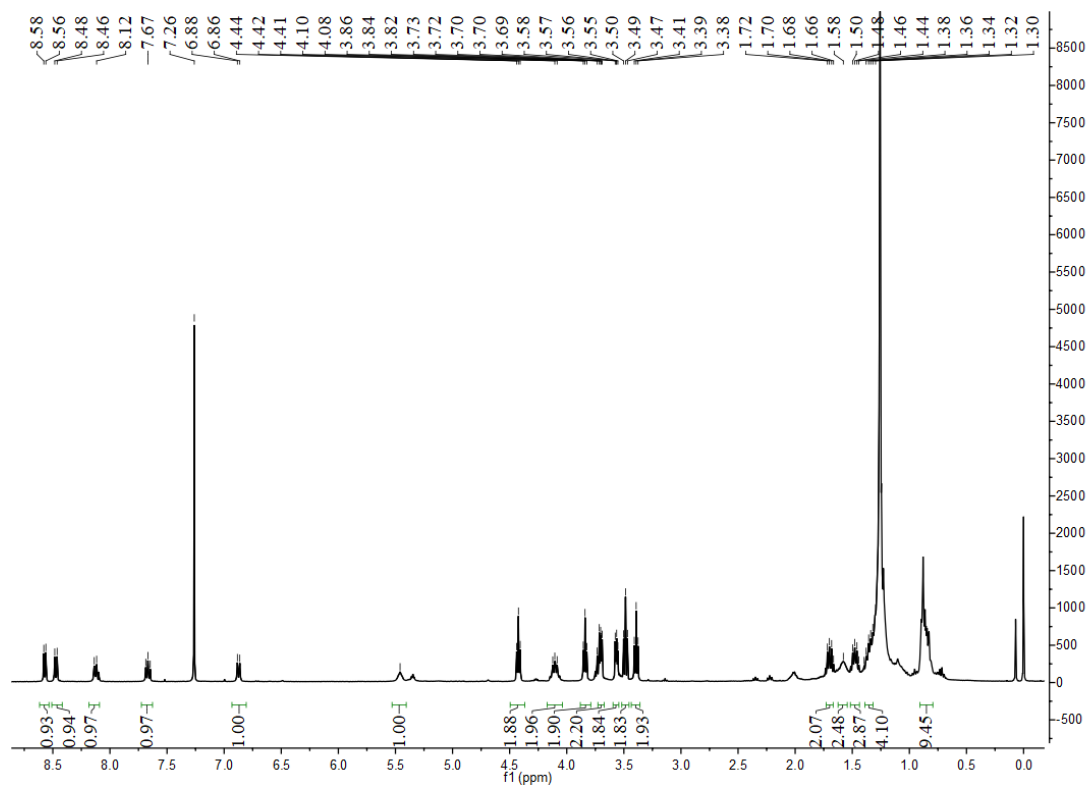


Fig. S43  $^1\text{H}$  NMR spectrum of TFEA-Naph-Halo in  $\text{CHCl}_3$ .

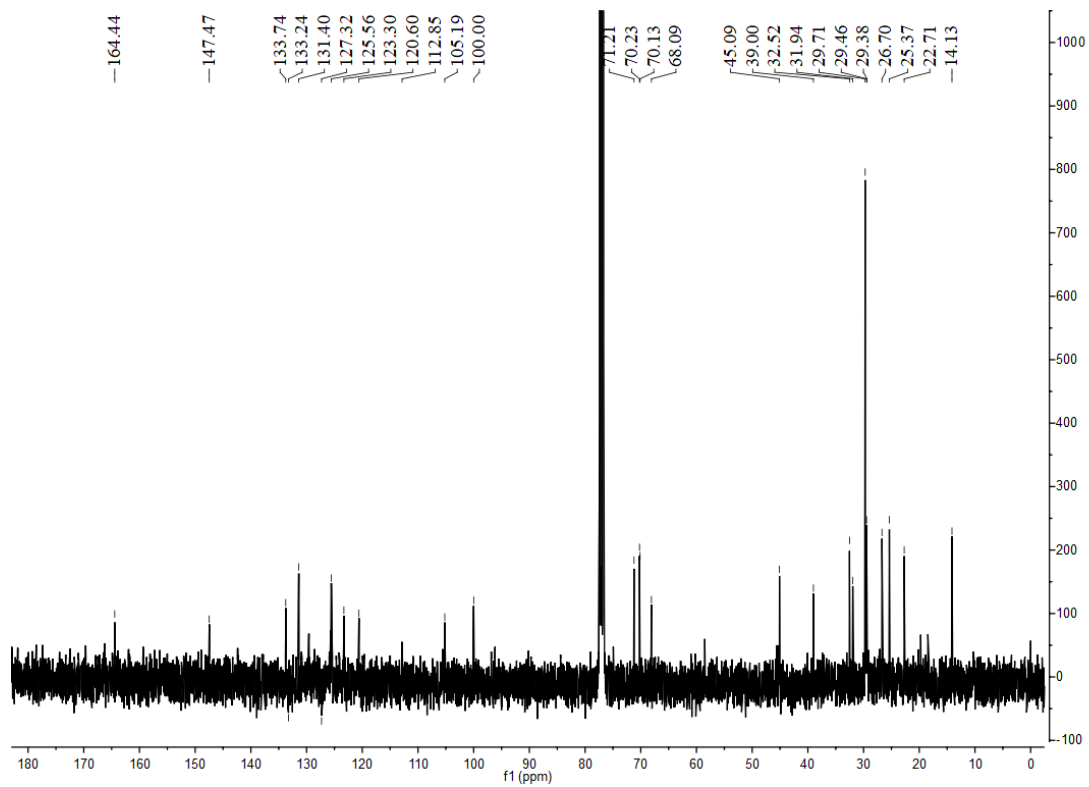


Fig. S44 <sup>13</sup>C NMR spectrum of TFEA-Naph-Halo in CHCl<sub>3</sub>.

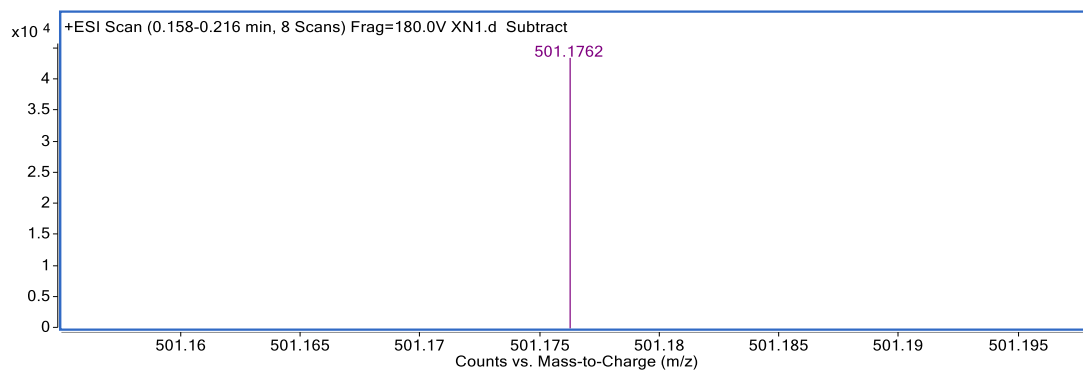


Fig. S45 HRMS spectrum of TFEA-Naph-Halo.